Modeling Cryptosporidium spp Oocyst Inactivation in Bubble-Diffuser Ozone Contactors

Special Project

LT ROBERT TOMIAK

JULY 1998

19981005 115

Modeling *Cryptosporidium* spp. Oocyst Inactivation in Bubble-Diffuser Ozone Contactors

Special Project

Robert Tomiak
LT, CEC, USN

University of Illinois at Urbana-Champaign
Department of Environmental Engineering

July 1998

DTIC QUALITY INSPECTED 4

Modeling *Cryptosporidium* spp. Oocyst Inactivation in Bubble-Diffuser Ozone Contactors

Robert B. Tomiak[1], Jason L. Rennecker[1], Benito J. Mariñas[1],
Richard J. Miltner[2], and James H. Owens[2]

[1]Department of Civil Engineering,
University of Illinois at Urbana-Champaign
Urbana, Illinois 61801

[2]National Risk Management Research Laboratory
U.S. Environmental Protection Agency,
Cincinnati, Ohio 45268

Introduction:

The CT concept (product of disinfectant concentration and characteristic contact time) is currently used to demonstrate compliance with disinfection requirements for *Giardia lamblia* (*G. lamblia*) and viruses under the Surface Water Treatment Rule (SWTR).[1] Minimum CT requirements include relatively large safety factors to account for possible deviations from actual disinfection efficiencies achieved in full-scale contactors. The application of this conservative regulatory approach for *Cryptosporidium parvum* (*C. parvum*) might result in unrealistic disinfection requirements under the Enhanced SWTR[2] due to the much stronger resistance of this protozoan parasite to inactivation by all chemical disinfectants used in drinking water applications. There is a need for the development of approaches that could provide a more accurate assessment of actual inactivation efficiency achieved in disinfection contactors.

The main objective of this study is to develop and apply a mathematical model for predicting the inactivation of *Cryptosporidium* spp. (*C. parvum* and *C. muris*) oocysts in ozone

bubble-diffuser contactors. The model is calibrated with semi-batch kinetic data, verified with pilot-scale inactivation experiments, and used for predicting and optimizing full-scale disinfection efficiency.

Background:

Waterborne pathogens pose a substantial public health risk if present in drinking water. One common goal of all potable water treatment plants, whose source is surface water, is the removal or inactivation of these pathogens. *Cryptosporidium* is perhaps the most resistant to disinfection efforts, and therefore it has been the subject of many studies and well founded concern. *Cryptosporidium* is classified as a coccidian protozoan parasite of both humans and animals.[3,4] Initially, as many as twenty species were named for the host in which they were found; however, subsequent studies indicated a lack of host specificity thereby invalidating many of the names. Two species affecting mammals, *Cryptosporidium parvum* (3.5μm diameter oocyst) and *Cryptosporidium muris* (5.8 μm diameter oocyst) have been identified. In addition, two other species, *C. baileyi* and *C. meleagridis*, are associated with birds. As the name suggests, *Cryptosporidium* denotes an organism with sporozoites concealed within an oocyst. As it has four aflagellar, but motile sporozoites with apical complexes, the genus *Cryptosporidium* has been assigned to the phyllum Apicomplexa, class Sporozoa.

Cryptosporidium was first identified in 1907 by Tyzzer after being observed in the gastric glands of asymptomatic laboratory mice.[5] It was not until 1976 that it was recognized as a

human pathogen by Nime.[6] Infection occurs after ingestion and also possibly by inhalation of the oocysts.[3,4] The oocysts are shed in the feces of infected humans or animals. Transmission occurs by person to person or animal to person contact; ingestion of contaminated food or water; or contact with contaminated objects. Once inside the intestinal tract, the oocysts reach the upper small bowel where proteolytic enzymes, bile salts, and temperature enhance the excystation of the four sporozoites. The sporozoites enter the brush border surface epithelium and develop into merozoites capable of replicating either asexually or sexually beneath the cell membrane in the brush border epithelial cell surface. Sexual stages combine to form new oocysts. The new oocysts have varyings shell thicknesses. Some of the oocysts generated with thinner than average shells may sporulate and continue to infect the same host, while the others are excreted. The cycle then continues, infecting other hosts.

Infection by *Cryptosporidium* is called Cryptosporidiosis.[3,4] The disease is characterized by copious, watery diarrhea; abdominal cramps; nausea; vomiting; anorexia; weight loss; flatulence; and fever. The incubation period is 2 to 14 days, with an average of 7 days. Recent studies suggest that the ID_{50}, the dose required to infect 50% of the subjects tested, is 132 oocysts. The real concern is that immunocompromised individuals are at increased risk. Immunocompromised individuals are young children, pregnant women, and people with a weakened immune system suffering from chronic illnesses such as HIV, hepatitis, renal failure and cancer. There is currently no known effective therapy for cryptosporidiosis. While the disease will typically run it's course in healthy victims, cryptosporidiosis in immocompromised individuals is chronic, progressive, and sometimes fatal. In pregnant women, cryptosporidiosis may result in birth defects, miscarriage or premature birth.

Cryptosporidiosis is most prevalent in underdeveloped countries where the sanitary systems are lacking and drinking water is not properly treated.[3,4] Numerous cases have also occurred in the United States. The most significant outbreak occurred in Milwaukee in April of 1993 and affected an estimated 403,000 people. Several immunocompromised patients died in what is now considered the largest waterborne outbreak in U.S. history. Undoubtedly, there have been many other outbreaks; however, due to the onset of symptoms which are very similar to those associated with a multitude of other diseases, many cases have most likely either gone unreported, or could not be confirmed.

The effective prevention of cryptosporidiosis is largely dependent upon the ability of individual water treatment plants to either render the oocysts nonviable, unable to sporulate and reproduce, through various treatment techniques, or to physically remove the oocysts from the water prior to distribution. While there has been an abundance of recent research regarding the chemical inactivation of *Cryptosporidium*, research is ongoing. The results currently appear to indicate that the only effective chemical agents are ozone and chlorine dioxide. Monochloramine and free chlorine species are generally considered ineffective under typical drinking water treatment conditions[7,8,9]. Physical separation of the oocysts from the water supply is possible through membrane filtration, and to a somewhat lesser extent through conventional sand filtration. Research to quantify the effectiveness of membrane filtration, as well as to identify a surrogate indicator that would be used in lieu of oocysts, is currently in progress. Numerous studies have documented the resistance of oocysts to extreme environmental conditions for

prolonged periods of time adding to the complexity and task of achieving inactivation to a degree suitable to prevent human infection.[10,11,12]

A substantial problem with modern treatment techniques is the inability for treatment plant operators to reliably measure viable oocysts in the drinking water they produce. There are a few techniques, flow cytometry and epifluorescent microscopy for example, available for counting oocysts in a given volume of water; however, there is no current technique for a plant operator to count oocysts leaving the plant and entering the water distribution system and distinguish between viable and inactivated oocysts.[13] Experimentally, there are currently two methods of assessing inactivation of viable *Cryptosporidium* spp. oocysts in water treatment systems.

The first viability assessment method is *in-vitro* excystation which involves exposing the oocysts to conditions that simulate the gastrointestinal environment of the host. Under the proper conditions, presumably only the oocysts which are still viable will excyst in accordance with their life cycle and release their four sporozoites. The technique is decribed in detail by Woodmansee (1987).[14] Until a recent contribution by Rennecker et al. (1997)[15], assessment of inactivation by *in-vitro* excystation was not very accurate due to the inability to differentiate between oocysts that were viable and had excysted, and those that appeared excysted but had really suffered damage due to over-exposure to ozone. After excystation is promoted, the viability efficiency can be accurately and reproducibly determined by counting the excysted sporozoites instead of the empty shells.

The second method is *in-vivo* or animal infectivity which involves the inoculation of animals, usually mice, with oocyst suspensions. The ID_{50} is determined using the Spearman-Karber method described by Finny (1978).[16] Inactivation is then determined by calculating the difference between the infection dose for exposed oocysts and an unexposed control. It is imperative that cross contamination of one animal by another does not occur, otherwise the data will be misinterpreted. This technique can be very time consuming and expensive, and can additionally be the subject of protest by animal activist groups.

Both methods, however, can be subject to error from many sources. Studies have indicated that different sample oocyst cleaning and preparation procedures may influence their resistance and viability thereby altering data sets run under the same conditions.[17] It is therefore potentially very important that experiments are conducted with the same batch of oocysts.

In accordance with the Safe Drinking Water Act (SDWA), the U.S. Environmental Protection Agency (U.S. EPA) has proposed the Enhanced Surface Water Treatment Rule (ESWTR) (U.S. EPA, 1994) which will require that water utilities provide average treatment efficiencies ranging from 99 to 99.9999% (2 to 6 logs) for *C. parvum* oocysts through filtration and disinfection. The impact to water utilities will be significant in that they will be forced to determine what modifications and additions to their water treatment plant are necessary, and then further demonstrate compliance. Of additional significance is that the U.S. EPA will have to provide technical guidance and develop a method of determining compliance with the proposed standard. To compound matters, the simplest and more accurate method is only realistically capable of assessing inactivation efficiencies up to 99.9% (3 logs). While the human benefit is

obvious, there does not presently exist a method of measuring the exact inactivation achieved by disinfection, so the implementation and enforcement of the proposed standard are inhibited by technological limitations at this point in time. The U.S. EPA unfortunately appears caught between the desire to protect the health of the population and the practicality of applying and enforcing needed regulations.

The drinking water industry is thus plagued with a human pathogen, *Cryptosporidium* spp., which appears to be present in most natural waters, happens to be very resistant to modern treatment techniques and is extremely difficult to measure. The federal agency charged with, among many other tasks, the protection of the health and well being of the population, has encountered a very delicate situation. They must promulgate standards which will ensure the safety of consumers, yet ensure that the capability exists to implement and enforce the standards. It is at this juncture that many new and exciting research efforts have originated in hopes of expanding the envelop of our understanding of *Cryptosporidium* and it's effective inactivation. A model accurately predicting oocyst inactivation could become a great tool for both regulators as well as plant designing engineers and operators.

Mathematical Model Development:

The use of ozone as a chemical disinfectant is becoming more common the drinking water industry. Recent research efforts have indicated that ozone is currently the most effective and safe chemical disinfectant for pathogens, requiring substantially less contact time to achieve

inactivation than chlorine, monochloramine and chlorine dioxide. The most common method of applying ozone is by diffusing it into water inside bubble-diffuser contactors of varying configurations. Bench scale experiments performed with batch and semi-batch reactors are being used to determine contact time and concentration required in order to achieve a specific level of inactivation for a pathogen of interest. There is currently no tool available, however, to measure the exact exposure time accrued in flow-through bubble-diffuser ozone contactors.

Currently, the CT concept is used to demonstrate compliance with disinfection requirements under the SWTR. Typically, a t_{10} hydraulic residence time is used to predict the contact time. This contact time will be conservative for most reactor designs except those approaching perfectly mixed (CSTR) conditions. The t_{10} hydraulic residence time is calculated from a non-reactive tracer test conducted on the contactor. It is defined as the period of time that it takes for 10% of the mass of a pulse input to reach the effluent, or alternatively for the effluent concentration to increase to 10% of the net concentration of a step input. The tracer test provides an indication of the amount of time that 90% of the oocysts entering the contactor at a given time will physically remain in the contactor. The t_{10} time is based on the mixing and dispersive characteristics of the ozone diffuser and chamber configuration. The t_{10} time is then multiplied by the average dissolved ozone concentration in a given chamber resulting in total CT. If research indicates that 5 minutes of "contact time" are required per mg/l of a known pathogen to achieve 3 logs (99.9%) of inactivation, the plant operator must ensure that the t_{10} time, which is fixed for a given contactor, multiplied by the average ozone concentration, results in 5 min-mg/l.

The plant operator is then left with the option of altering the quantity of ozone injected into the chamber as the sole means of achieving a desired level of inactivation. This approach is conservative and may additionally result in unrealistic disinfection requirements specifically for *C. parvum* under the ESWTR due to the much stronger resistance of this pathogen to inactivation by all chemical disinfectants used in drinking water applications. Equally challenging is the design phase of an ozone contactor. The designer can modify height, diameter, diffuser type, add additional chambers, split the ozone input over two or more different chambers, specify counter or co-current flow, and alter the liquid and gas flow rates. While the designer has software available to predict impacts on cost and physical performance, there is no existing tool with which performance related to inactivation of pathogens can be evaluated.

The intent of the model developed in this study is to provide a basis for making sound decisions about the design and operation of ozone contactors in an effort to achieve a desired goal of pathogen inactivation. The model is formulated from mass balance principles incorporating contactor hydrodynamic information obtained from tracer tests, experimentally measured pathogen inactivation, ozone decomposition and mass transfer kinetics. The hydrodynamics inside the contactor chambers are assumed to approach ideal axial dispersion reactor (ADR) conditions. The mass balance equations provide an accurate prediction of the dissolved ozone concentration profile throughout a given chamber. The designer may select either counter or co-current flow on which to base the contactor. Counter current as implied, is a chamber in which ozone gas enters from the bottom and the water enters from the top. Both ozone gas and liquid influent enter from the bottom in a co-current chamber. Any number of additional chambers can represented. Ozone may be applied in any chamber. If no ozone is

applied in a given chamber, the chamber simply becomes reactive, in which the dissolved ozone exiting the previous chamber is allowed to continue decomposing, meanwhile providing additional contact time with the microorganisms with perhaps less back mixing.

The equations representing the calculations of all basic parameters required for any configuration are given in Appendix I. Using the model, an operator may input the physical dimensions and flow rates of his or her current plant including chamber height and diameter, water temperature and density, liquid and gas flow rates, concentration of ozone applied, and the dispersion characteristics (dispersion number) of the contactor. The dispersion number is the ratio of liquid diffusivity to the liquid velocity and chamber height and represents the extent of physical mixing within the contactor. If the dispersion number is unknown, it may be estimated from tracer data using an iterative process employing the Thomas Method.[18] This technique is demonstrated later when a contactor owned by the U.S. EPA Research Laboratory in Cincinnati is modeled in order to compare the results and accuracy of this model's predictions.

The designer is at liberty to create virtually any dimensions and parameters in order to observe the impact on inactivation achieved. Both users, the designer as well as the operator, must be careful to account for the ozone demand in the influent water, a parameter which may easily vary with season, rain events, or organic matter concentration. Every body of water will have a natural ozone demand based primarily on the organic content of the water. Designers must be sure to use an ozone decomposition rate applicable to the body of water under worse conditions under which the contactor is to operate. Last, any pathogen can be modeled, provided

its inactivation kinetics are known. The user is referred to previously published inactivation rates for a specific pathogen of interest.

The equations resulting from a mass balance on a counter-current chamber configuration are derived in detail in Appendix II. The overall mass balance equation on the liquid side is represented by:

$$\frac{\partial C_L}{\partial t} = E_L \cdot \frac{\partial^2 C_L}{\partial X^2} - \frac{U_L}{\varepsilon} \cdot \frac{\partial C_L}{\partial X} + K_L \cdot a \cdot \left(C_L^* - C_L\right) - K_D \cdot C_L \qquad (1)$$

The equation accounts for turbulent diffusivity, advection, mass transfer from the gas to the liquid phase governed by the Two Film Mechanism and Henry's Law, and the decomposition of the ozone in the liquid phase. The liquid volume fraction, ε, can be taken as approaching unity for typical drinking water conditions, and the corresponding steady-state equation can be partially non-dimensionalized to:

$$d\frac{\partial^2 C_L}{\partial Z^2} - \frac{\partial C_L}{\partial Z} + N_L \cdot \left(\frac{C_G}{m} - C_L\right) - N_D \cdot C_L = 0 \qquad (2)$$

The overall mass balance equation on the gas side is represented by:

$$\frac{\partial C_G}{\partial t} = E_G \cdot \frac{\partial^2 C_G}{\partial X^2} + \frac{U_G}{1-\varepsilon} \cdot \frac{\partial C_G}{\partial X} - \frac{\varepsilon}{(1-\varepsilon)} \cdot K_L \cdot a \cdot \left(C_L^* - C_L\right) - K_D \cdot C_G \qquad (3)$$

The equation accounts for turbulent diffusivity, advection, mass transfer from the gas to the liquid phase, and the decomposition of the ozone in the gas phase. Making the assumptions that diffusivity and reactivity of ozone in the gaseous phase are negligible, assuming steady state, taking the liquid volume fraction, ε, as approaching unity, and non-dimensionalizing each term, the equation can be reduced to:

$$\frac{\partial\left(\frac{C_G}{m}\right)}{\partial Z} - \frac{N_L}{S}\left(\frac{C_G}{m} - C_L\right) = 0 \qquad (4)$$

Equations 2 and 4 can be solved after applying Danckwert's[19] boundary conditions and the known ozone gas input at the contactor bottom. The solution provides the following expression for the dissolved ozone profile through the contactor:

$$C_L(Z) = \left(EXP(\lambda_1 Z) - \frac{S}{N_L}\lambda_1 EXP(\lambda_1 Z)\right)\alpha_1 + \left(EXP(\lambda_2 Z) - \frac{S}{N_L}\lambda_2 EXP(\lambda_2 Z)\right)\alpha_2 + \left(EXP(\lambda_3 Z) - \frac{S}{N_L}\lambda_3 EXP(\lambda_3 Z)\right)\alpha_3 \qquad (5)$$

This profile will be important and used later in predicting pathogen inactivation throughout a contactor chamber. Appendix III indicates the development of equations resulting from a mass balance on a co-current chamber configuration. Similarly, Appendix IV indicates the development of equations resulting from a mass balance on a reactive chamber. The equation representing a reactive chamber is simplified since there is no mass balance on the gas. The

mass balance on the liquid will contain only advection and reaction terms if plug flow conditions are assumed. At this juncture, it should be noted that the reactive chamber mass balance equations can additionally be utilized in the predicted performance of a contacting basin, such as a chlorine contactor, where the introduction of a gas is not an issue.

With a complete profile of dissolved ozone throughout every chamber in an ozone contactor, a mass balance on the pathogen of interest can be performed. The resulting equations are derived in detail and presented in Appendix V. The overall mass balance on the pathogen is represented by:

$$\frac{\partial N}{\partial t} = E_L \cdot \frac{\partial^2 N}{\partial X^2} - U_L \cdot \frac{\partial N}{\partial X} - K_N \cdot N \cdot C_L \qquad (6)$$

The equation accounts for turbulent diffusivity, advection, and the inactivation reaction of the pathogen with ozone. If steady state is assumed, and the equation is partially non-dimensionalized, the equation can be reduced to:

$$d \cdot \frac{\partial^2 N}{\partial Z^2} - \frac{\partial N}{\partial Z} - N_N \cdot N \cdot C_L = 0 \qquad (7)$$

The dependence of pathogen inactivation on dissolved ozone concentration is readily apparent. Since the concentration of dissolved ozone is not constant throughout the chamber, an iterative finite element approach is taken. The resulting tri-diagonal matrix can be solved by the

Thomas Method. Finally, an expression is derived for the inactivation of the pathogen which accounts for the history of exposure through a changing ozone profile.

The reaction term is represented by the Chick-Watson Law of pseudo-first order inactivation kinetics.[20] The Chick-Watson Law can be applied in the case of *C. muris*, as its' inactivation conforms to that of a pseudo-first order reaction. However, the Chick-Watson Law may not be applicable to all pathogens, in which case, the correct mathematical or empirical relationship should be used. Chen (1998)[21] devised an ingenious method to account for the inactivation of a pathogen which indicates a "shoulder" profile. An example is *C. parvum* which, as indicated by Rennecker et al. (1997)[15], displays a resistance to ozone until a certain amount of contact time is exceeded, then follows the Chick-Watson first order reaction rate kinetics. Chen (1998)[21] recommends linear regression of the inactivation profile that does conform with a first order reaction rate in order to find a theoretical starting amount of pathogens, N/N_0, higher than 100%. With the proper programming statements, the model can represent any amount of pathogens calculated to be greater than 100% as only 100%, indicating no achieved inactivation. The model would then display a "shoulder", or period of no inactivation, until the first order rate law would take effect and begin indicating pathogen amounts of less than 100%. This technique is demonstrated later when a contactor owned by the U.S. EPA Research Laboratory in Cincinnati is modeled in order to compare results and accuracy of this model's predictions with the experimental inactivation of *C. parvum*.

The equations developed in Appendices I through V are ideal for spreadsheet application where graphs can be used for a visual representation of both the dissolved ozone and pathogen

inactivation profiles. The spreadsheet provides a user-friendly, easy way of inputting and altering design and operational parameters and observing the inactivation achieved. The model can then be used to evaluate the effectiveness of any configuration on the inactivation of a pathogen of interest. The designer can optimize performance while the operator can understand the impact of altering operational parameters. This model combines the results of extensive research with the mathematical characteristics of the application and provides a useful tool which summarizes anticipated performance.

Measuring Model Accuracy:

In order to validate this model, experimental data from Owens et al. (1994)[22] was used. Owens and co-workers, employed by the U.S. Environmental Protection Agency Research Laboratory in Cincinnati, Ohio, have conducted several experiments with their pilot scale bubble diffuser depicted by Figure 1. Their single chamber ozone contactor measures 2.65 meters in height and 0.15 meters in diameter and is operated in the counter-current configuration. It has sampling ports at the influent and effluent, as well as at four intermediate locations spaced equally at 0.46 meters apart. The ozone was produced from oxygen by a model GL-1 generator made by PCI, Inc. The concentration of ozone applied to the contactor and that released in the off- gas was measured by ultra violet (UV) light. The difference in the two measurements gave the amount of ozone transferred to the liquid. The transfer efficiency was estimated to be greater than 94%. Additionally, the ozone demand was estimated by measuring the ozone concentration in the effluent at the last sampling port and subtracting it from the ozone transferred. The liquid

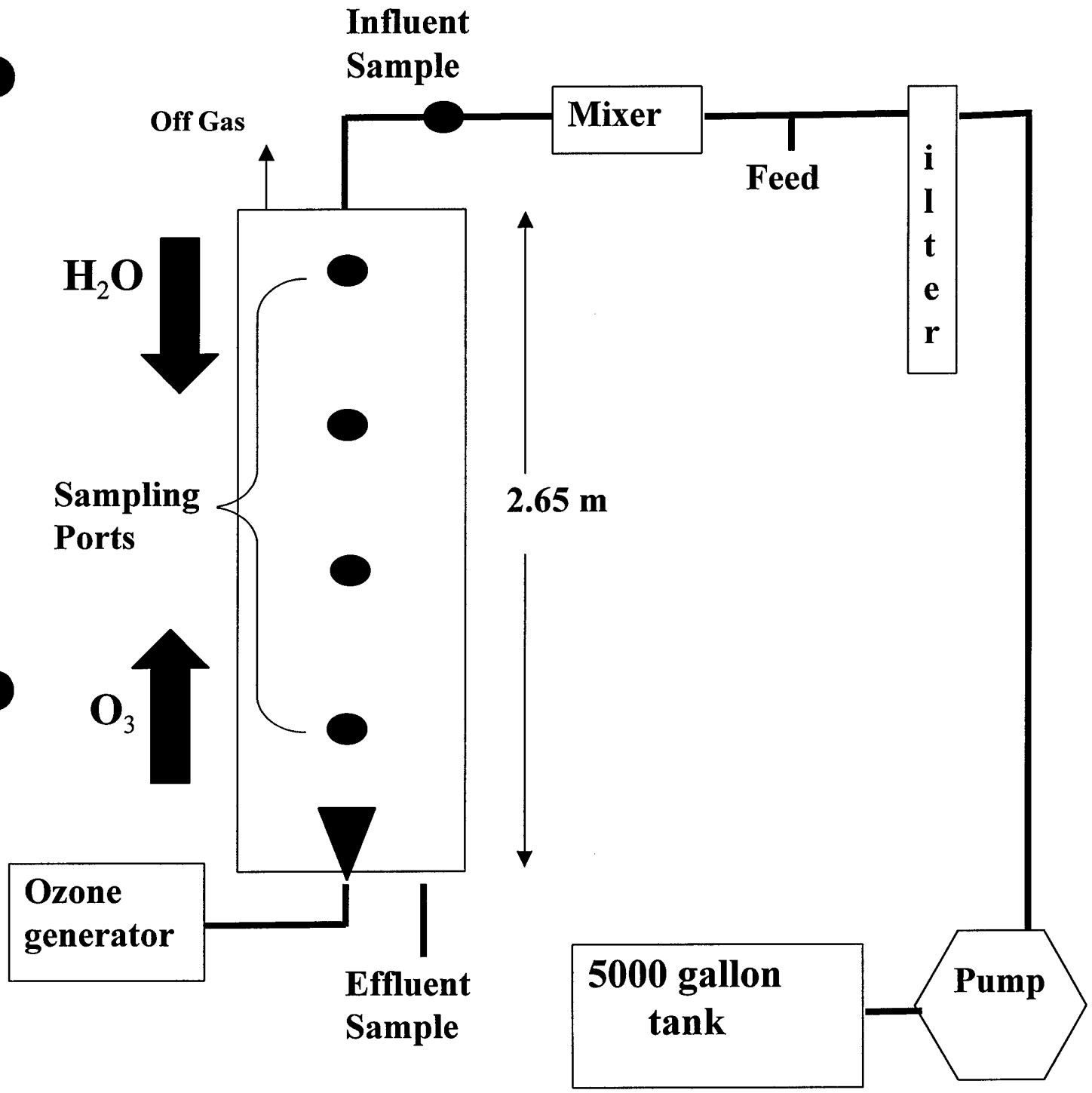

Figure 1

Diagram of pilot-scale ozone contactor

and gas flow rates used were 6.4 L/min and 0.64 L/min, respectively. Step dose tracer studies revealed a theoretical mean residence time, T_{Θ}, of 7.4 minutes and a T_{10} time of 2.27 minutes. Filtered Ohio River water was used throughout all experiments. Experimantal conditions were a temperature of 22-25°C, pH of 7.5-8.5, and a total organic content (TOC) of 1.61 to 2.08 mg/L.

Oocysts were obtained from various sources, *Giardia muris* from the University Hospital in Cleveland Ohio from female mice, *Cryptosporidium muris* from Japan's Osaka University, Medical School also from female mice, and *Cryptosporidium parvum* from a locally infected Holstein calf. A suspension of 100 oocysts/mL was fed at 2mL/minute into the filtered Ohio River water, just ahead of the contactor. Samples were then collected at the various ports within the contactor and assayed via both *in vitro* excystation and animal infectivity. They were then able to display inactivation profiles through the contactor from data generated from the excystation and/or infectivity assays.

Comparing the predictions of the mathematical model to the results obtained experimentally will presumedly validate the accuracy of the model. A few parameters required to run the model were not specifically known, and thus had to be either derived or empirically calculated. First, while the transferred ozone concentration was determined, the actual percentage of pure ozone applied at the bottom of the contactor was not known. By using a simple mass balance:

$$Q_G * (C_{G\,IN} - C_{G\,OUT}) = Q_L * C_L \qquad (8)$$

and by assuming the transfer efficiency of "greater than 94%" was 97%, effectively reducing the maximum possible error in calculation to 3%, $C_{G\,OUT}$ could be calculated to be 0.03 $C_{G\,IN}$. Knowing the transferred ozone concentration, C_L, $C_{G\,IN}$ could be determined with the following relationship for each of the three levels of reported transferred ozone:

$$C_{G\,IN} = \frac{Q_L}{Q_G} * C_L * \frac{1}{0.97} \qquad (9)$$

Additionally, the dispersion number for the contactor was unknown. However, since the tracer tests produced T_Θ and T_{10} times, the ratio, T_{10}/T_Θ could be calculated to be 0.3068. Using the Thomas Method, described in detail in Appendix V, trial values for d, the dispersion number, can be generated until the resulting profile indicates a T_{10}/T_Θ value of 0.3068. Trial and error results in a dispersion number of 0.4424 which can be used to model the EPA's contactor. The Thomas Method is very useful and is commonly used as a tool to integrate tracer concentrations over time to arrive at a step profile.

Last, the model applies a known ozone demand to predict inactivation. Since ozone demand is a temperature dependent reaction term, the data accumulated by Owens et al. must be translated into a reaction coefficient, K_D. Recall the equation given by Appendix II for the liquid side:

$$\frac{\partial C_L}{\partial t} = E_L \cdot \frac{\partial^2 C_L}{\partial X^2} - \frac{U_L}{\varepsilon} \cdot \frac{\partial C_L}{\partial X} + K_L \cdot a \cdot \left(C_L^* - C_L\right) - K_D \cdot C_L \qquad (10)$$

In this case, since the dissolved ozone concentration in the contactor effluent was reported, the reaction coefficient, K_D, can be altered until the proper resulting values of dissolved ozone effluent concentration is properly matched by the model. Table 1 summarizes all relevant parameters.

At this point, the model has all the parameters required to predict a dissolved ozone concentration profile throughout the contactor. Additionally, if the kinetic reaction term, K_N, applicable to a given pathogen is known, the model will predict an inactivation profile for the pathogen throughout the contactor. Inactivation of pathogens are given by the Chick-Watson pseudo-first order reaction rate: K_N*N*C_L, where K_N is the second reaction rate constant, N is the count of active, viable oocysts at a given point in the contactor, and C_L is the corresponding dissolved ozone concentration at that point. *C. muris* conforms ideally to this pseudo-first order reaction. Unfortunately, previous research documented by Rennecker et al. (1997)[15] only accounted for the inactivation of *C. muris* through a temperature range between 5 and 20 °C, while the experiments completed by Owens et al. (1994)[22] were conducted at 22 to 25 °C. Rennecker et al. (1997)[15] suspected that above 20 °C, the inactivation coefficient increased at a much greater rate than the temperature dependency indicated between 5 and 20 °C. By following the same procedures outlined in Rennecker et al. (1997)[15], additional experiments were conducted with *C. muris* which has provided a temperature dependent inactivation coefficient valid through 30 °C represented by the following expression:

C. muris Experimental Data (Owens et al. 1994)

Transferred Ozone (mg/L)	Contactor Effluent (mg/L)	Ozone Demand (mg/L)	Reaction Constant K_D	Log Inactivation
1.03	0.37	0.66	.416	0.41
1.37	0.32	1.05	.867	0.51
1.38	0.34	1.04	.789	0.36
2.07	1.22	0.85	.129	1.20
2.11	1.26	0.85	.124	1.58
2.76	1.54	1.22	.154	1.64
3.31	1.87	1.44	.148	2.56
3.72	2.05	1.67	.160	>2.70
4.63	2.53	2.10	.165	>2.62

Temperature: 23.6 +/- 1.6 °C

C. parvum Experimental Data (Owens et al. 1994)

Transferred Ozone (mg/L)	Contactor Effluent (mg/L)	Ozone Demand (mg/L)	Reaction Constant K_D	Log Inactivation
1.58	0.71	0.87	.262	1.08
1.76	0.88	0.89	.198	0.57
2.71	1.46	1.25	.163	1.80
3.20	1.69	1.51	.173	2.17
3.31	1.81	1.50	.157	1.95
3.56	1.71	1.84	.2205	2.67
3.97	2.35	1.46	.124	>2.90
4.17	2.31	1.86	.152	>2.15

Temperature: 24.5 +/- 1.6 °C

Table 1

Experimental parameters

$$K_N = EXP(12.5)\ X\ EXP\left(-\frac{33500}{8.314 \times T}\right), \text{ where temperature is in °K} \qquad (11)$$

When this relationship is used, the model predicts inactivation per Figure 2. Data from Owens et al. (1994)[22] is depicted also to illustrate the close match between experimental and model predicted inactivation.

Some pathogens, *C. parvum* for example, may not ideally conform to the Chick-Watson first order inactivation rule. *C parvum* actually indicates a shoulder, a period of no inactivation with ozone exposure until a certain contact time threshold is exceeded. After reaching the threshold, the first order inactivation rate is applicable. Figure 3 indicates the inactivation profile for *C. parvum*. If the linear portion of the inactivation profile, that which does comply with a first order rate law, is projected upwards to an intercept above N/N_O=100, the entire profile can be modeled as first order, per Figure 4. This means that the model can be used to simulate a starting pathogen count of higher than 100% and make use of the Chick-Watson first order law to predict the entire profile. With some logic built into the programming, the model can ignore all inactivation, N/N_O, profile calculations predicted to be in excess of 100 and simply let N/N_O=100 for those data points. In this manner, the model can account for a "shoulder". Work by Rennecker et al. (1997)[15] has provided a temperature dependent inactivation coefficient for *C. parvum* represented by:

$$K_N = 1.2985\ X\ 10^{15}\ EXP\left(-\frac{10079.4}{T}\right), \text{ where temperature is in °K.} \qquad (12)$$

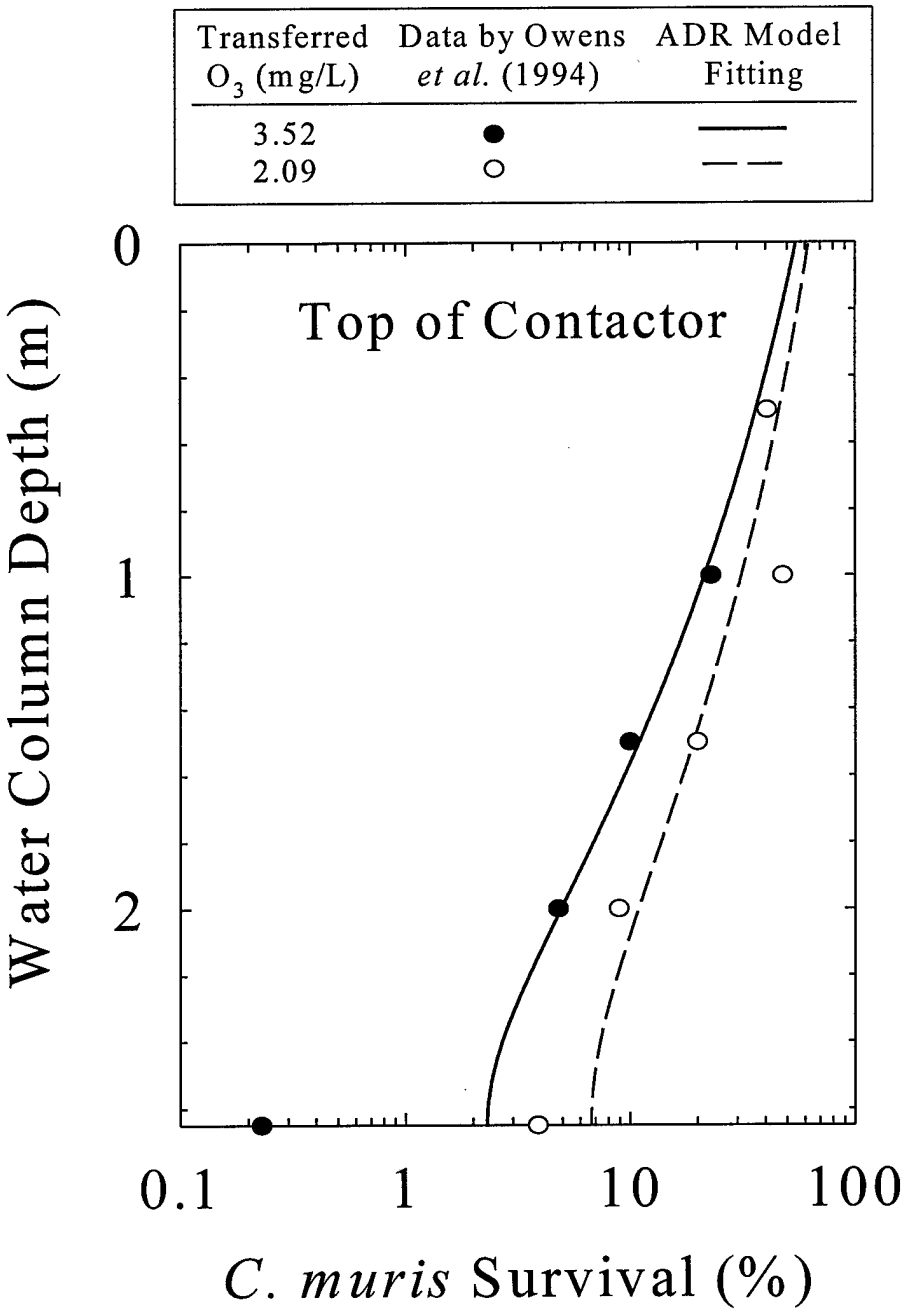

Figure 2

Comparison of model predicted to experimentally determined inactivation of *C. muris*

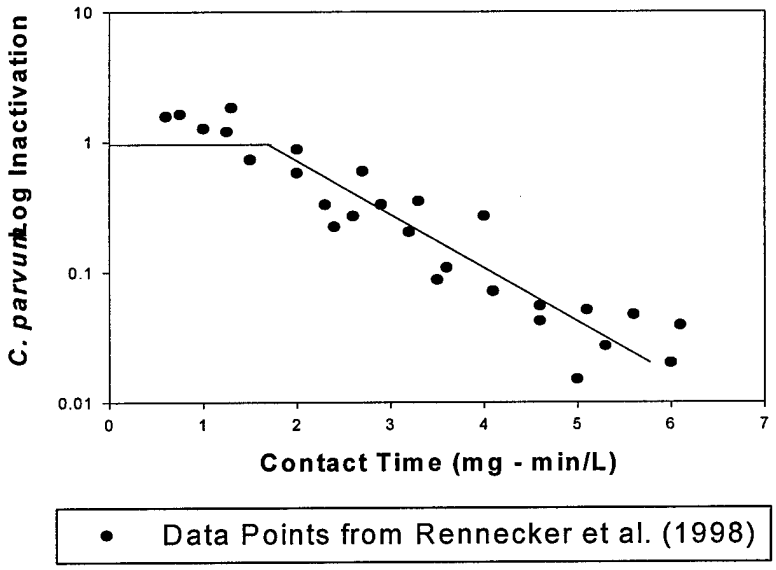

Figure 3

Experimental data from Rennecker et al (1998) depicting the shoulder trend observed with *C. parvum*. Shoulder signifies a required contact time prior to any observed inactivation beginning

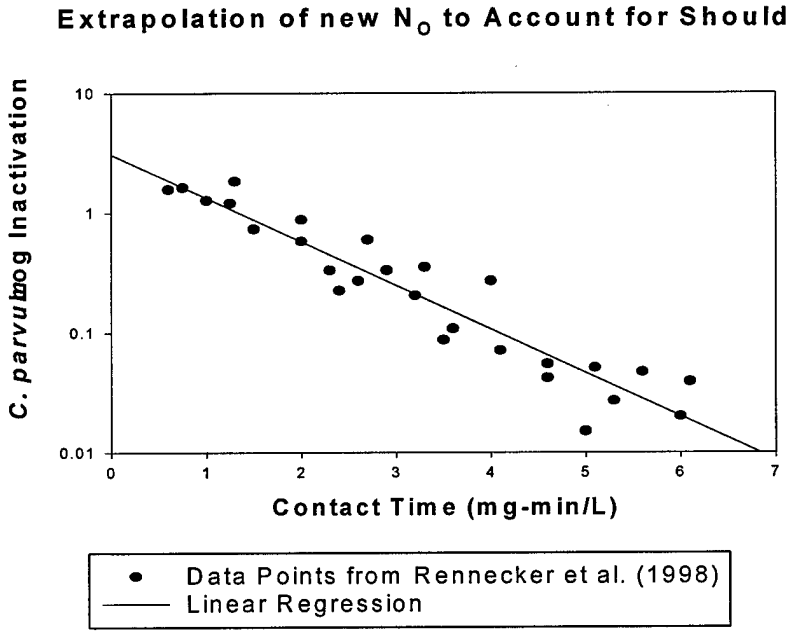

Figure 4

By linear regression, a new N/N_0 is obtained in order to make use of the entire linear profile

When this relationship is used, the model predicts inactivation per Figure 5. Data from Owens et al. (1994)[22] is depicted also to illustrate the close match between experimental and model predicted inactivation.

As can be observed from Figures 2 and 5, the model predicts inactivation very accurately as compared to the inactivation measured experimentally by Owens et al. (1994)[22]. Discrepancies can be attributed to many factors inherent in any experiment. First, the exact temperature of the Ohio River water was not known, but rather a range was provided. This is not viewed as a significant error because the model can simulate the relatively small range and predict a corresponding "range" of inactivation which, when done, would be rather small. Second, the ozone demand for a given body of water will vary significantly from month to month and following rain events. The experiments run by Owens et al. (1994)[22] were conducted over a period of a few months, necessitated by the scarcity of available oocysts and the physical duration of excystation and infectivity tests. Third, an empirical dispersion number was generated, in lieu of knowing the specific contactor dispersive characteristics. Fourth, the tests conducted by Owens et al. (1994)[22] can measure with a certain degree of accuracy up to 2 logs of inactivation when using the excystation method, however, beyond that point lose reliability. Effectively, to measure for example 3 logs of inactivation (99.9%) by excystation, a count of 8000 oocysts is required to obtain a statistically accurate answer. Last, removing samples from ports within a contactor and ensuring that quenching occurs immediately is critical. Otherwise, residual dissolved ozone may continue to effect the oocysts, even briefly, resulting in an

ADR Model Fitting of *C. parvum* Oocyst Inactivation Data

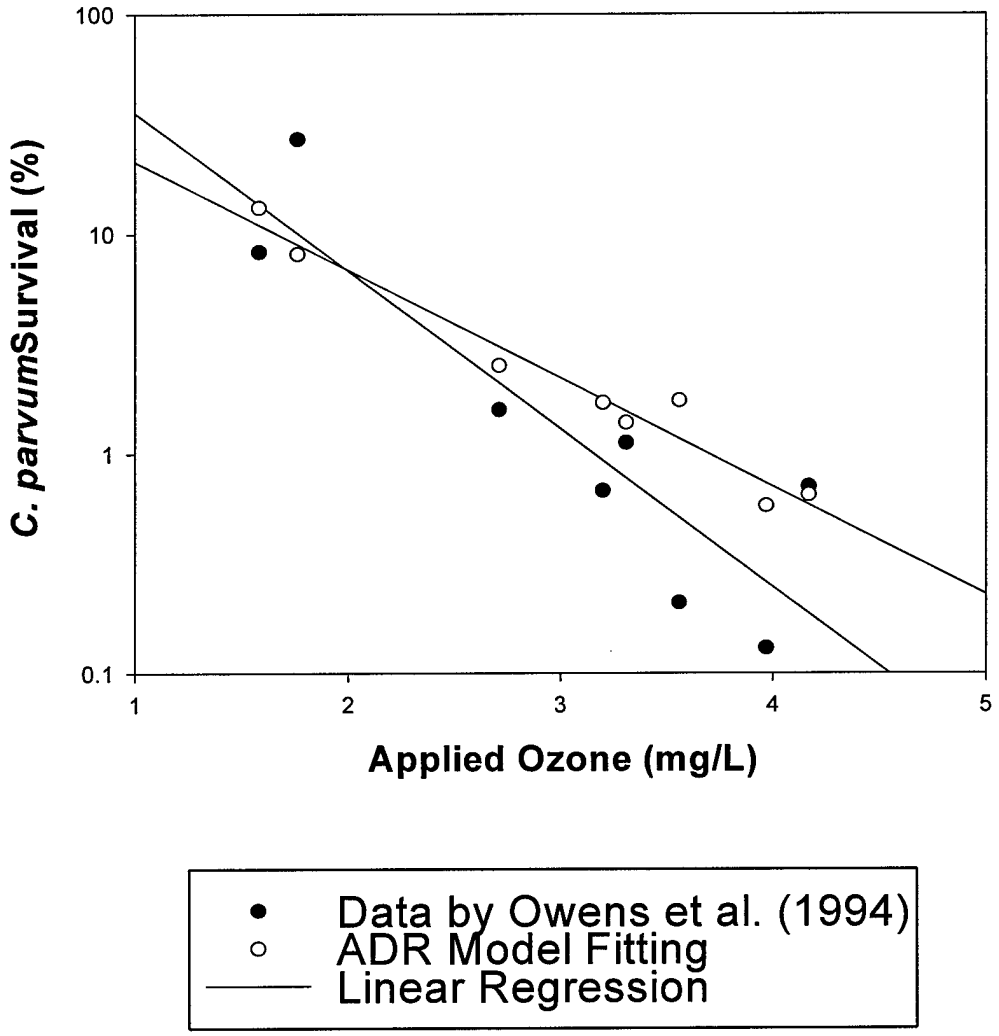

Figure 5

Comparison of model predicted to experimentally determined inactivation of *C. parvum*

overestimation of inactivation. Additionally, if the sampling port comes off a pipe even a few inches long, plug flow conditions with high dissolved ozone concentrations, especially at the bottom sampling ports, may likewise induce an overestimation of inactivation.

Taking into account all the possible inaccuracies, the model predicts extremely well compared to the experimental data of Owens et al. (1994)[22], which to date is really the only known available data with which to verify the model. The observed margin of difference between the experimental and model predictions is on the order of magnitude of less than 1%. The model's predictions are certainly within the range of accuracy suitable to forego expensive and time consuming experimental tests, which are themselves, inherently subject to error.

Model Applications:

With the model set up on a spreadsheet, the applications become endless. The designer of a bubble-diffuser ozone contactor is at liberty to alter almost any parameter and observe the resultant effect on inactivation predicted. The plant operator who is managing an existing contactor in operation is somewhat restricted, however, they can still significantly alter the inactivation by a few very important parameters. The usefulness of the model in optimizing plant efficiency can be observed by a few examples.

To begin with, the bubble-diffuser can be designed as a simple one chamber system, however, it may be configured for counter-current or co-current. Using the dimensions and operating parameters of the contactor previously described, the model was run for various applied ozone concentrations. As depicted by Figure 6, in each case, higher inactivation was achieved for the co-current configuration. Changes to the height and diameter of the chamber did not change the result. The verdict is that if a single chamber model is desired, it should be configured for co-current operation.

If multiple chambers are desired, the results are interestingly not as predictable. For chambers all of equal diameter, the counter-current configuration achieves higher inactivation compared to the co-current configuration at varying concentrations of applied ozone per Figure 7. When the chamber diameters are altered such that chambers one and three are larger, 15 cm for example, and chambers two, four, five and six are smaller, 5 cm for example, the counter-current configuration can be optimized and achieves higher inactivation for the same concentrations of applied ozone. Figure 8 indicates the observed inactivation corresponding to the two configurations. By viewing the concentration of dissolved ozone in the effluent of the sixth chamber, it can be seen that there is a slightly higher concentration of ozone in the effluent of the co-current configuration. It would seem that a lower inactivation is achieved potentially due to more of the ozone not being utilized. The counter-current configuration results in a slightly smaller dissolved ozone concentration in the effluent indicating more efficient use of the ozone towards inactivation.

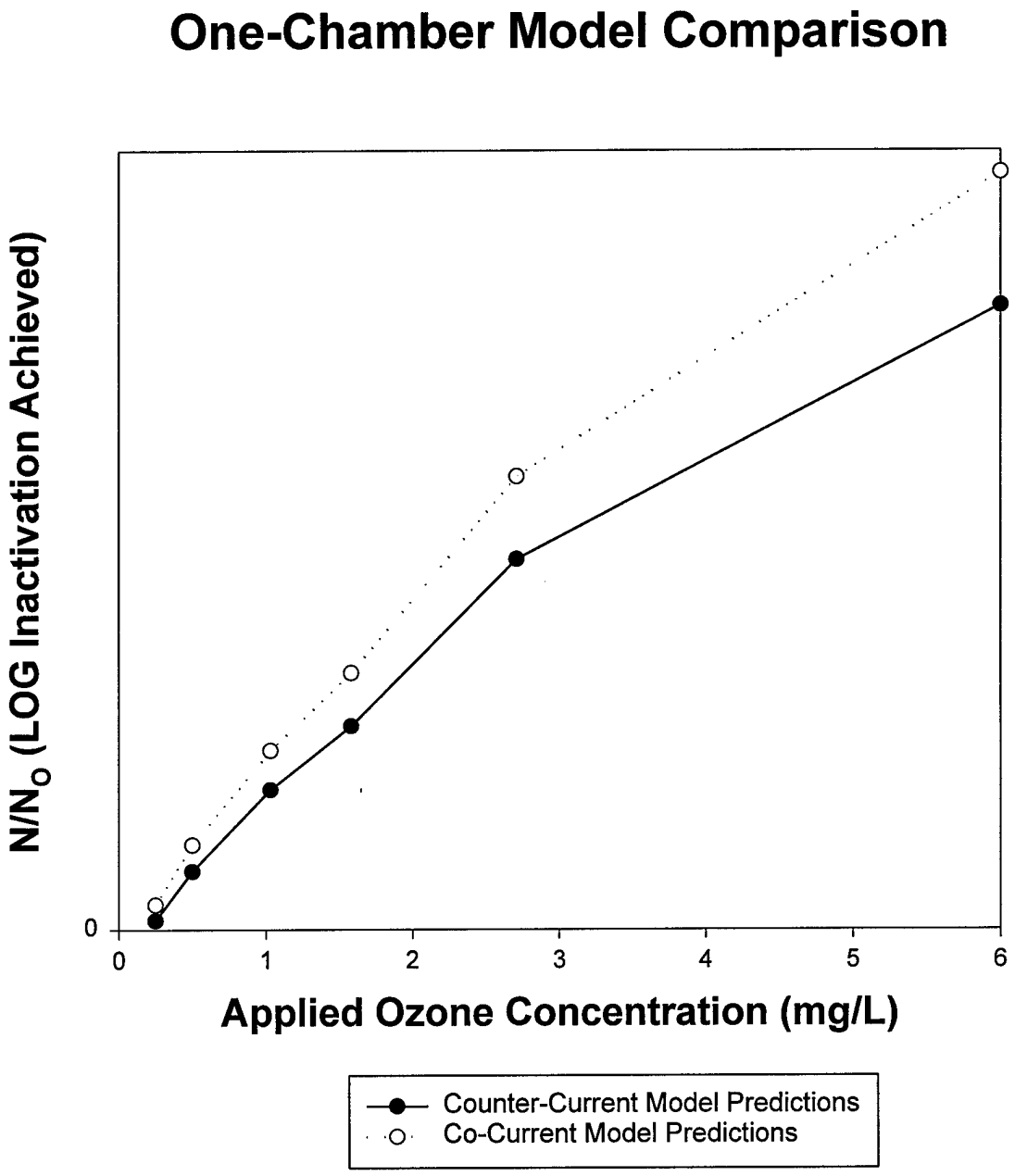

Figure 6

Comparison of inactivation effectiveness of one-chamber design configurations

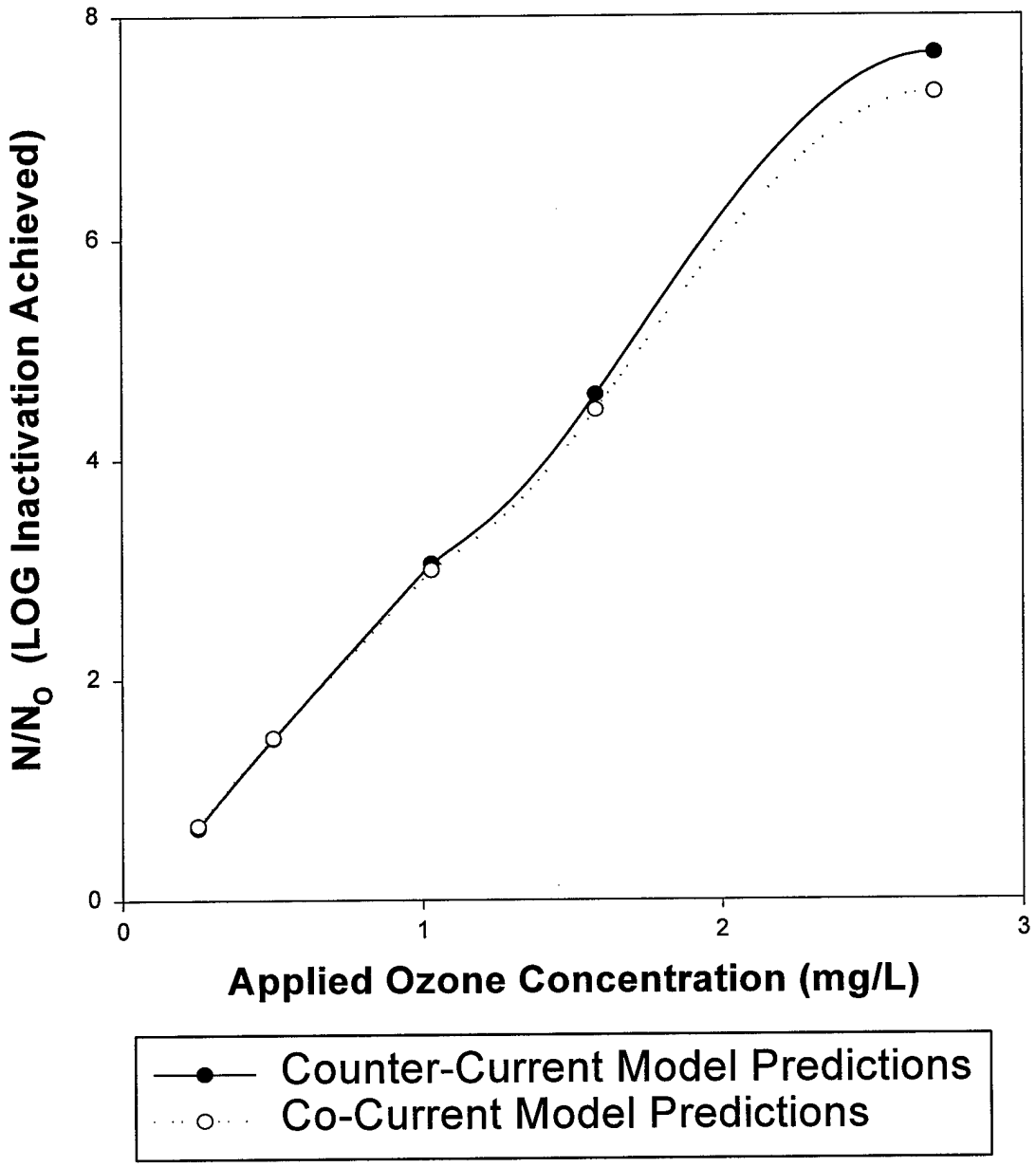

Figure 7

Comparison of inactivation effectiveness of multi-chamber, constant diameter design configurations

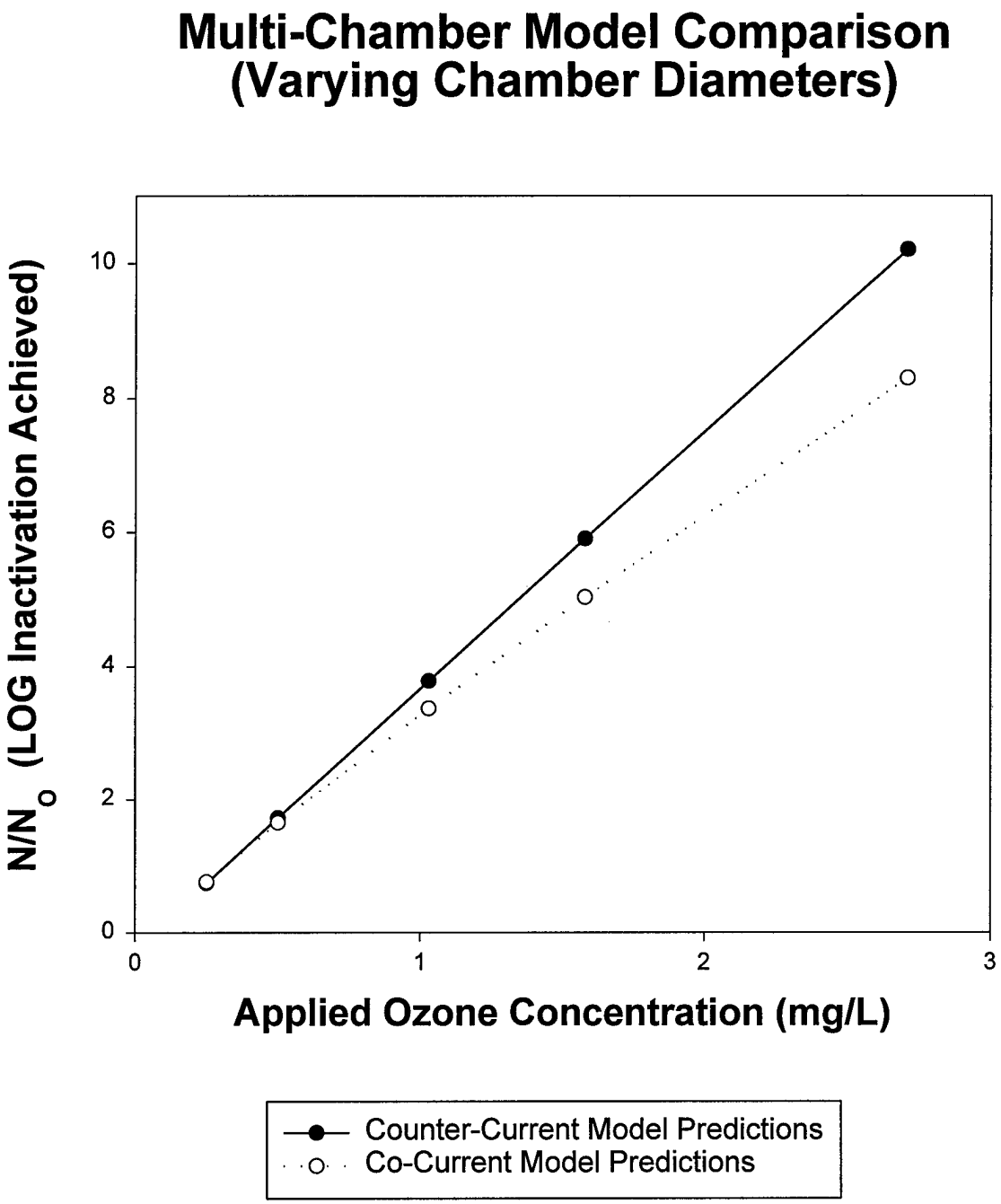

Figure 8

Comparison of inactivation effectiveness of multi-chamber, variable diameter design configurations

As is frequently the case, many multi-chamber bubble diffusers permit split ozone input. To accomodate and predict the efficiency of these designs, the model allows for the input of ozone in chambers one and three. The interpretation of the results in the comparison of both configurations is not as obvious. For varying concentrations of ozone applied, and varying chamber diameters, the co-current model achieved highest inactivation consistently when 100% of the ozone was applied in the first chamber. While not performing as well as the co-current configuration, the counter-current configuration indicated that inactivation can be maximized with a 75/25 % split ozone input between chambers one and three if dispersion was assumed in the reactive chambers. When assuming no dispersion occurs in the reactive chambers, plug flow conditions prevail and inactivation can be maximized with a 25/75 % split ozone input between chambers one and three. This only held true in the case where the chamber diameters were equal and there was an indication that the ozone was depleted too much when 100% was applied in the first chamber to make effective use of the last chamber. Again, the results indicated that the level of inactivation was related to the efficient use of dissolved ozone so that neither high nor very low concentrations were observed in the effluent from the final chamber. A high final chamber effluent concentration indicated a waste of ozone while a low effluent concentration indicated a waste of a chamber.

Seasonal fluctuations in temperature, as may be imagined, could pose a substantial impact to plant efficiency. The exact relationship of temperature dependence is another factor which is not inherently obvious and the model may be of great assistance. Using data and parameters reported by Owens et al. (1994)[22], it may be observed that an increase in temperature results in greater inactivation of *C. parvum* per Figure 9. This is not a result which should be

taken as a conclusive trend in every case. It is possible that specific sources of drinking water may have large seasonal variations in organic content. If the ozone reaction or degradation coefficient is adjusted to reflect increasing organic content with higher, summer temperatures, it is possible that ozone demand, if excessive, could actually result in lower inactivation. The conclusion is thus not as predictable without the help of the model and accounting for the conditions inherent to the specific water source. The designer and operator must account for ozone demand in the influent water before making decisions based on temperature alone. With the model, the operator may make an intelligent decision to either increase or reduce the amount of applied ozone as the seasonal temperature and ozone demand changes in order to consistently meet inactivation requirements.

The results obtained when modifying a few parameters are interesting and not readily predictable. They indicate that the operator, while physical dimensions and parameters can not be altered, has a wide range of flexibility and can indeed optimize the plant's efficiency regarding pathogen inactivation. A designer has unlimited flexibility, and if specifically aware of the influent characteristics, temperature and ozone demand, can make very wise engineering decisions regarding plant configuration, number of chambers, applied ozone, flow rates and physical dimensions. Coupled with a software that optimizes cost, the designer can specify the most cost and performance efficient plant, or best value for the customer.

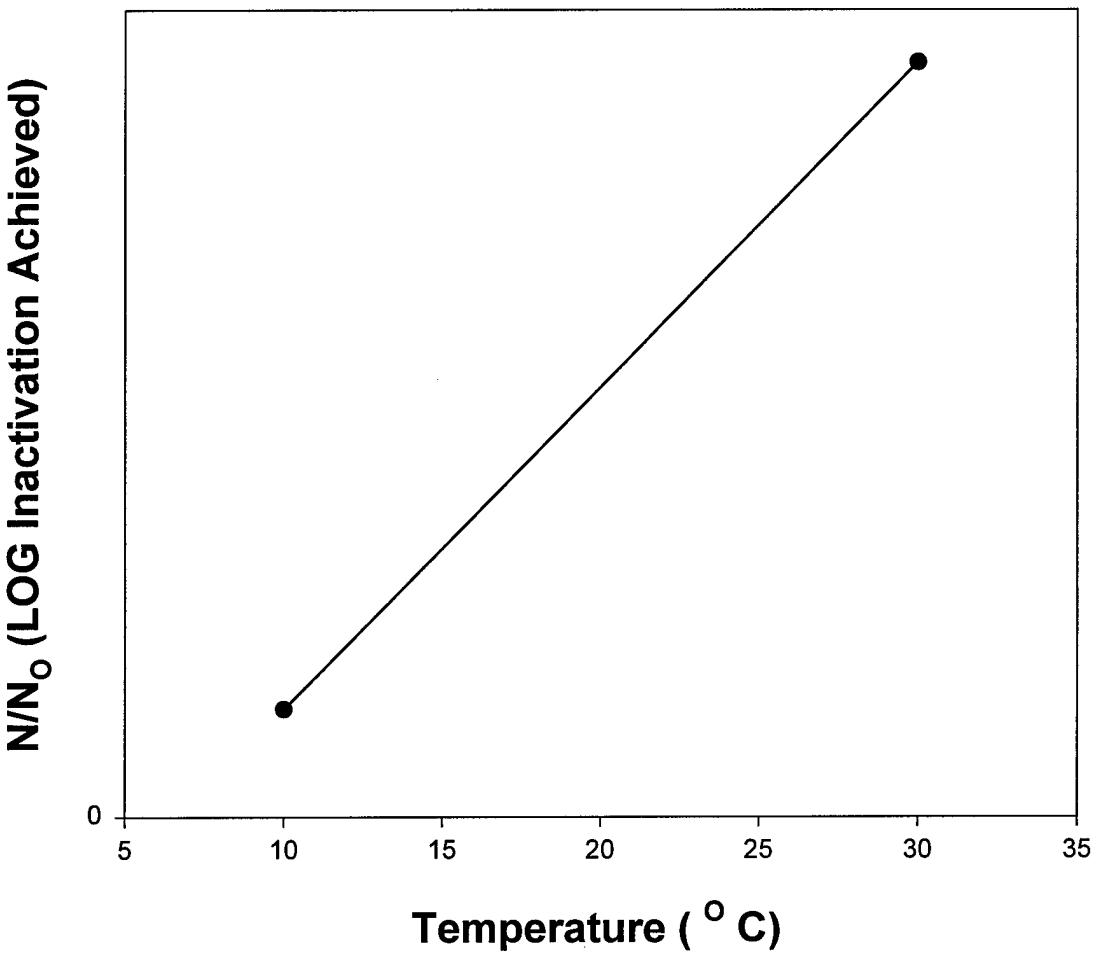

Figure 9

Effect of temperature on inactivation effectiveness on *C. parvum* in Ohio River water

Conclusion:

There is a need for a method of predicting and optimizing inactivation of pathogens in drinking water treatment plants. In the interest of public health, new, more stringent standards must be implemented, achieved, and enforced. The design and operation of a bubble-diffuser ozone contactor should not be strictly based on comfort, cost or tradition. As more is discovered about *Cryptosporidium* spp., disinfection and filtration should jointly and intelligently be utilized to achieve the 99.9999% inactivation level desired. The model described in this paper is based on mass balance principles and has been validated by experimental results. When incorporated in a spreadsheet type software, the equations take the form of a simple, user-friendly application with graphically displayed results. It provides predictions of dissolved ozone concentrations and the corresponding pathogen inactivation which could be reasonably anticipated for a given set of physical characteristics and operating parameters with a very high level of accuracy. The application to design and operation of bubble-diffuser ozone contactors is unlimited and at a minimum provides excellent guidance and recommendations in order to achieve optimum inactivation.

References

1. USEPA, National Primary Drinking Water Regulations: Filtration, Disinfection, Turbidity, *Giardia lamblia*, Viruses, *Legionella*, and Heterotrophic Bacteria; Final Rule, Federal Register, 54:124:27486 (June 29, 1989).

2. USEPA, National Primary Drinking Water Regulations: Enhanced Surface Water Treatment Requirements; Proposed Rule, Federal Register, 59:145:38832 (July 29, 1994).

3. Guerrant, Richard L. (1997) "Cryptosporidiosis: An Emerging, Highly Infectious Threat". *Emerging Infectious Diseases*, 3(1),1-9.

4. Current, William L. (1986) "*Cryptosporidium*: Its Biology and Potential for Environmental Transmission". *CRC Critical Reviews in Environmental Control*, 17(1), 21-51.

5. Tyzzer, E.E. (1907) "A sporozoan found in the peptic glands of the common mouse". *Proc. Soc Exp Biol Med*, the protozoan 5, 12-13.

6. Nime, F.A., Burek, J.D., Page, D.L., Holscher, M.A. and Yardley, J.H. (1976) "Acute entercolitis in a human being infected with *Cryptosporidium*". *Gastroenterology*, 70, 592-598.

7. Ransome, M.E., Whitmore, T.N. and Carrington, E.G. (1993) "Effect of disinfectants on the viability of *Cryptosporidium parvum* oocysts". *Water Supply*, 11, 103-117.

8. Korich, D.G., Mead, J.R., Madore, M.S., Sinclair, N.A. and Sterling, C.R. (1990) "Effects of Ozone, Chlorine Dioxide, Chlorine, and Monochloramine on *Cryptosporidium parvum* Oocyst Viability". *Applied and Environmental Microbiology*, 56(5), 1423-1428.

9. Finch, G.R., Black, E.K., Gyurek, L. and Belosevic, M. (1993) "Ozone Inactivation of *Cryptosporidium parvum* in Demand-free Phosphate Buffer Determined by In Vitro Excystation and Animal Infectivity". *Applied and Environmental Microbiology*, 59(12), 4203-4210.

10. Fayer, Ronald (1994) "Effect of High Temperature on Inactivity of *Cryptosporidium parvum* Oocysts in Water". *Applied and Environmental Microbiology*, 60(8), 2732-2735.

11. Fayer, Ronald and Nerad, Thomas (1996) "Effects of Low Temperatures on Viability of *Cryptosporidium parvum* Oocysts". *Applied and Environmental Microbiology*, 62(4), 1431-1433.

12. Robertson, L.J., Campbell, A.T. and Smith, H.V. (1992) "Survival of *Cryptosporidium parvum* Oocysts under Various Environmental Pressures". *Applied and Environmental Microbiology*, 58(11), 3494-3500.

13. Vesey, G., Slade, J.S., Byrne,M., Shepherd, K., Dennis, P.J. and Fricker, C.R. (1993) "Routine Monitoring of *Cryptosporidium* Oocysts in Water using flow cytometry". *Journal of Applied Bacteriology*, 75, 87-90.

14. Woodmansee, Douglas B. (1987) "Studies of In Vitro Excystation of *Cryptosporidium parvum* from calves". *J. Protozool*, 34(4), 398-402.

15. Rennecker, Jason L., Mariñas, Benito J., Rice, Eugene W. and Owens, James H. (1997) "Kinetics of *Cryptosporidium parvum* Oocyst inactivation with ozone". *Proceedings of the 1997 American Water Works Association Water Technology Conference*, June 15-19, 1997, Atlanta, Ga, 299-316.

16. Finney, D.J. (1978) "Statistical method in biological assay, 3rd ed, p 394-401. Macmillan Publishing Co., Inc. New York.

17. Campbell, A.T., Robertson, L.J. and Smith, H.V. (1993) "Effects of Preservatives on Viability of *Cryptosporidium parvum* Oocysts". *Applied and Environmental Microbiology*, 59(12), 4361-4362.

18. Chapra, S.C. and Canale, R.P. (1988) *Numerical Methods for Engineers*. 2d ed., McGraw-Hill, New York.

19. Dankwerts, P. (1953). "Continuous flow systems: distribution of residence times". *Chemical Engrg Sci*, 2(1), 1-13.

20. Chick, H. (1908) "An investigation of the laws of disinfection". *J. Hyg*, 8, 92-158.

21. Chen, J. (In progress) "PhD Doctoral" Purdue University

22. Owens, J.H., Miltner, R.J., Schaefer III, F.W. and Rice, Eugene, W. (1994) "Pilot-Scale Inactivation of *Cryptosporidium* and *Giardia*". *Proceedings of the 1994 American Water Works Association Water Technology Conference*, November 6-10, 1994, San Francisco, Ca, 1319-1328.

Appendix

Appendix I. Notation and General Calculations

Symbol	Definition	Formula
A	Chamber Area (cm^2)	$\Pi \times \frac{D^2}{4}$
a	Effective Area (cm^{-1})	$\frac{6 \times U_G}{d_B(V_B - U_L)}$
C_L	Concentration of ozone in liquid phase (mg/L)	
C_L^*	Interfacial ozone concentration (mg/L)	
C_G	Concentration of ozone in the gas phase (mg/L)	
D	Chamber Diameter (cm)	
d	Dispersion Number	$\frac{E_L}{U_L \cdot L}$
d_B	Average Gas Bubble Diameter (cm)	$d_{BO} + 0.21 U_G$
d_{BO}	Gas Bubble Diameter at Diffuser Outlet (cm)	
E_G	Turbulent Gas Diffusivity (cm^2/sec)	
E_L	Turbulent Liquid Diffusivity (cm^2/sec)	$6E-8 \times \frac{T}{\mu_L}$

G_{in}	**Percent of Ozone in Applied Gas by Weight**	
K_D	**Ozone Decomposition Rate (sec^{-1})**	$1.808E14 \times Exp\left(\frac{-9746}{286.15}\right)$
K_L	**Liquid Mass Transfer Coefficient (cm/sec)**	$\frac{S_h \times D_L}{d_B}$
K_{OL}	**Overall Mass Transfer Coefficient (cm/sec)**	
K_N	**Inactivation Constant for Pathogen (mg/L-min)**	
L	**Chamber Height (m)**	
m	**Henry's Constant**	$\text{Log (m)} = 3.25 - \frac{840}{T}$
M	**Mass (mg)**	
N	**Quantity of Oocysts**	
N_D	**Dimensionless Ozone Decomposition Rate**	$\frac{K_D \cdot L}{U_L}$
N_L	**Dimensionless Mass Transfer Coefficient**	$\frac{K_L \times a \times L}{U_L}$
N_N	**Dimensionless Inactivation Constant for Pathogen**	$\frac{K_N \cdot L}{U_L}$
Q_G	**Gas Flow Rate (L/min)**	
Q_L	**Liquid Flow Rate (L/min)**	

r_c	**Mass reaction rate (mg/L)**	
r_L	**Mass transfer rate (mg/L)**	
R_e	**Reyolds Number**	$\frac{V_B \times d_B}{\nu_L}$
S_c	**Schmidt Number**	$\frac{\nu_L}{D_L}$
S_h	**Shaffer Number**	$2 + .0187\left[R_e^{.484} \times S_c^{.339} \times \left(\frac{d_B \times 980^{.333}}{D_L^{.667}}\right)^{.072}\right]^{1.61}$
s	**Stripping Factor**	$\frac{m \cdot Q_G}{Q_L}$
t	**Time (sec)**	
T	**Temperature (°K)**	t + 273.15
T	**Temperature (°F)**	
U_G	**Gas Flow Velocity (cm/sec)**	$\frac{Q_G}{A}$
U_L	**Liquid Flow Velocity (cm/sec)**	$\frac{Q_L}{A}$
μ_L	**Dynamic Viscosity (centipoise)**	$\frac{100}{2.1482 \times \left(t - 8.4385 + \sqrt{80784 + \left(t - 8.435\right)^2}\right) - 120}$
V_B	**Bubble Rise Velocity (cm/sec)**	$210 \times d_B \times \frac{1.004}{\mu}$
ν	**Kinematic Viscosity (cm^2/sec)**	$\frac{\mu_L}{\rho_L}$
X	**Length (cm)**	

Z	**Dimensionless Length Coefficient**
Δ	**Denotes "change in" the associated variable**
∂	**Denotes "infinitesimal change in" the associated variable**
ε	**Liquid Volume Fraction**
Φ	**Mass Flux**
Θ	**Dimensionless Time Coefficient**

Appendix II. Mass Balance for Counter-Current Ozone Chamber

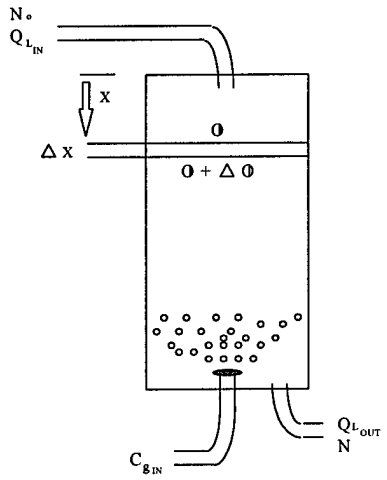

Liquid Side:

Mass Accumulation = Mass In – Mass Out + Mass Reacted + Mass Transferred

$$\Delta M = \Phi - (\Phi + \Delta\Phi) + V \cdot r_L + V \cdot r_C$$

$$\Delta M = C_L \cdot A \cdot \varepsilon \cdot \Delta X$$

$$\Phi = -E_L \cdot A \cdot \varepsilon \cdot \frac{\Delta C_L}{\Delta X} + Q_L \cdot C_L$$

$$r_L = K_{OL} \cdot a \cdot \varepsilon \cdot \left(C_L^* - C_L\right)$$

$$r_C = -K_D \cdot \varepsilon \cdot C_L$$

So the equation becomes:

$$\Delta(\Delta M) = -\Delta\Phi \cdot \Delta t + V \cdot r_L \cdot \Delta t + V \cdot r_C \cdot \Delta t$$

$$\Delta C_L A\varepsilon \cdot \Delta X = \left(E_L A\varepsilon \frac{\Delta^2 C_L}{\Delta X} - Q_L \Delta C_L \right)\Delta t + A\varepsilon \cdot \Delta X \cdot K_{OL} a\left(C_L^* - C_L\right)\Delta t - A\varepsilon \cdot \Delta X \cdot K_D C_L \Delta t$$

Dividing through by $A \cdot \varepsilon \cdot \Delta X \cdot \Delta t$ results in:

$$\frac{\Delta C_L}{\Delta t} = E_L \cdot \frac{\Delta^2 C_L}{\Delta X^2} - \frac{Q_L}{A \cdot \varepsilon} \cdot \frac{\Delta C_L}{\Delta X} + K_{OL} \cdot a \cdot \left(C_L^* - C_L\right) - K_D \cdot C_L$$

Taking the limit as the delta becomes infinitely small, $\Delta \rightarrow 0$, and additionally substituting K_L for K_{OL} since the mass transfer resistance on the gas side is negligible results in:

$$\frac{\partial C_L}{\partial t} = E_L \cdot \frac{\partial^2 C_L}{\partial X^2} - \frac{U_L}{\varepsilon} \cdot \frac{\partial C_L}{\partial X} + K_L \cdot a \cdot \left(C_L^* - C_L\right) - K_D \cdot C_L$$

To non-dimensionalize the equation, multiply each term by $\frac{L}{U_L}$:

$$\frac{L}{U_L} \cdot \frac{\partial C_L}{\partial t} = \frac{E_L \cdot L}{U_L} \cdot \frac{\partial^2 C_L}{\partial X^2} - \frac{U_L \cdot L}{\varepsilon \cdot U_L} \cdot \frac{\partial C_L}{\partial X} + \frac{K_L \cdot a \cdot L}{U_L} \cdot \left(C_L^* - C_L\right) - \frac{K_D \cdot L}{U_L} \cdot C_L$$

Non-dimensionalized coefficients will be defied as follows:

$$\Theta = \frac{t \cdot U_L}{L} \qquad N_L = \frac{K_L \cdot a \cdot L}{U_L}$$

$$Z = \frac{X}{L} \qquad N_D = \frac{K_D \cdot L}{U_L}$$

$$d = \frac{E_L}{U_L \cdot L} \qquad C_L^* = \frac{C_G}{m}$$

The non-dimensionalized equation then becomes:

$$\frac{\partial C_L}{\partial \Theta} = d \cdot \frac{\partial^2 C_L}{\partial Z^2} - \frac{1}{\varepsilon} \cdot \frac{\partial C_L}{\partial Z} + N_L \cdot \left(\frac{C_G}{m} - C_L\right) - N_D \cdot C_L$$

If the contactor is allowed to reach steady-state, then $\frac{\partial C_L}{\partial \Theta} = 0$ and:

The mass balance for the liquid side becomes:

$$d \cdot \frac{\partial^2 C_L}{\partial Z^2} - \frac{1}{\varepsilon} \cdot \frac{\partial C_L}{\partial Z} + N_L \cdot \left(\frac{C_G}{m} - C_L\right) - N_D \cdot C_L = 0$$

Gas Side:

Mass Accumulation = Mass In – Mass Out + Mass Reacted + Mass Transferred

$$\Delta M = C_G \cdot A \cdot (1-\varepsilon) \cdot \Delta X$$

$$\Phi = -E_G \cdot A \cdot (1-\varepsilon) \cdot \frac{\Delta C_G}{\Delta X} - Q_G \cdot C_G$$

$$r_L = K_L \cdot a \cdot \varepsilon \cdot (C_L^* - C_L)$$

$$r_C = -K_D \cdot (1-\varepsilon) \cdot C_L$$

So the equation becomes:

$$\Delta(\Delta M) = -\Delta\Phi \cdot \Delta t + V \cdot r_L \cdot \Delta t + V \cdot r_C \cdot \Delta t$$

$$\Delta C_G A(1-\varepsilon) \cdot \Delta X = \left(E_G A(1-\varepsilon) \frac{\Delta^2 C_G}{\Delta X} + Q_G \Delta C_G \right) \Delta t + A(1-\varepsilon) \cdot \Delta X \cdot K_L a (C_L^* - C_L) \Delta t - A(1-\varepsilon) \cdot \Delta X \cdot K_D C_G \Delta t$$

Dividing through by $A \cdot (1-\varepsilon) \cdot \Delta X \cdot \Delta t$ results in:

$$\frac{\Delta C_G}{\Delta t} = E_G \cdot \frac{\Delta^2 C_G}{\Delta X^2} + \frac{Q_G}{A \cdot (1-\varepsilon)} \cdot \frac{\Delta C_G}{\Delta X} - \frac{\varepsilon}{(1-\varepsilon)} K_L \cdot a \cdot (C_L^* - C_L) - K_D \cdot C_G$$

Taking the limit as the delta becomes infinitely small, $\Delta \to 0$ results in:

$$\frac{\partial C_G}{\partial t} = E_G \cdot \frac{\partial^2 C_G}{\partial X^2} + \frac{U_G}{1-\varepsilon} \cdot \frac{\partial C_G}{\partial X} - \frac{\varepsilon}{(1-\varepsilon)} \cdot K_L \cdot a \cdot (C_L^* - C_L) - K_D \cdot C_G$$

To non-dimensionalize the equation, multiply each term by $\frac{L}{U_L}$:

$$\frac{L}{U_L} \cdot \frac{\partial C_G}{\partial t} = \frac{E_G \cdot L}{U_L} \cdot \frac{\partial^2 C_G}{\partial X^2} + \frac{U_G \cdot L}{(1-\varepsilon) \cdot U_L} \cdot \frac{\partial C_G}{\partial X} - \frac{K_L \cdot a \cdot L \cdot \varepsilon}{(1-\varepsilon) \cdot U_L} \cdot (C_L^* - C_L) - \frac{K_D \cdot L}{U_L} \cdot C_G$$

The non-dimensionalized equation then becomes:

$$\frac{\partial C_G}{\partial \Theta} = \frac{E_G}{U_L \cdot L} \cdot \frac{\partial^2 C_G}{\partial Z^2} + \frac{U_G}{U_L \cdot (1-\varepsilon)} \cdot \frac{\partial C_G}{\partial Z} - \frac{N_L \cdot \varepsilon}{(1-\varepsilon)} \cdot (C_L^* - C_L) - N_D \cdot C_G$$

If the contactor is allowed to reach steady-state, then $\frac{\partial C_G}{\partial \Theta} = 0$.

Additionally, considering that diffusivity in the gas bubbles is extremely small and ozone is non-reactive in air, we can eliminate two additional terms.

The mass balance for the gas side becomes:

$$\frac{U_G}{U_L \cdot (1-\varepsilon)} \cdot \frac{\partial C_G}{\partial Z} - \frac{N_L \cdot \varepsilon}{(1-\varepsilon)} \cdot \left(C_L^* - C_L\right) = 0$$

Since $C_L^* = \frac{C_G}{m}$, and $S = \frac{m \cdot U_G}{U_L}$, the equation becomes,

$$\frac{S}{(1-\varepsilon)} \cdot \frac{\partial\left(\frac{C_G}{m}\right)}{\partial Z} - \frac{\varepsilon}{(1-\varepsilon)} \cdot N_L \cdot \left(\frac{C_G}{m} - C_L\right) = 0$$

Now we have two equations representing our system. Assuming $\varepsilon \cong 1$ for ozone, the two equations reduce to the final form:

I. $$d\frac{\partial^2 C_L}{\partial Z^2} - \frac{\partial C_L}{\partial Z} + N_L \cdot \left(\frac{C_G}{m} - C_L\right) - N_D \cdot C_L = 0$$

II. $$\frac{\partial\left(\frac{C_G}{m}\right)}{\partial Z} - \frac{N_L}{S}\left(\frac{C_G}{m} - C_L\right) = 0$$

Using the boundary conditions:

Liquid:

$$C_L(Z=0) = C_{L,IN} + d\frac{\partial C_L}{\partial Z}\Big|_{Z=0} \quad \text{(Inlet)}$$

$$\frac{\partial C_L}{\partial Z}\Big|_{Z=1} = 0 \quad \text{(Outlet)}$$

Gas:

$$C_G(Z=1) = C_{G,IN}$$

If in Equation II, we let $Y = \frac{C_G}{m}$, we get:

$$\frac{\partial Y}{\partial Z} - \frac{N_L}{S}(Y - C_L) = 0$$

We can rearrange and solve for C_L in terms of Y as follows:

$$C_L = Y - \frac{S}{N_L} \cdot \frac{\partial Y}{\partial Z}$$

With an expression for C_L in terms of Y, we can develop expressions for the first and second derivatives of C_L as follows:

$$\frac{\partial C_L}{\partial Z} = \frac{\partial Y}{\partial Z} - \frac{S}{N_L} \cdot \frac{\partial^2 Y}{\partial Z^2} \qquad \text{and}$$

$$\frac{\partial^2 C_L}{\partial Z^2} = \frac{\partial^2 Y}{\partial Z^2} - \frac{S}{N_L} \cdot \frac{\partial^3 Y}{\partial Z^3}$$

Substitution into Equation I results in:

$$d\left(\frac{\partial^2 Y}{\partial Z^2} - \frac{S}{N_L} \cdot \frac{\partial^3 Y}{\partial Z^3}\right) - \left(\frac{\partial Y}{\partial Z} - \frac{S}{N_L} \cdot \frac{\partial^2 Y}{\partial Z^2}\right) + N_L\left[Y - \left(Y - \frac{S}{N_L} \cdot \frac{\partial Y}{\partial Z}\right)\right] - N_D\left(Y - \frac{S}{N_L} \cdot \frac{\partial Y}{\partial Z}\right) = 0$$

or

$$d\frac{\partial^2 Y}{\partial Z^2} - d \cdot \frac{S}{N_L} \cdot \frac{\partial^3 Y}{\partial Z^3} - \frac{\partial Y}{\partial Z} + \frac{S}{N_L} \cdot \frac{\partial^2 Y}{\partial Z^2} - S \cdot \frac{\partial Y}{\partial Z} - N_D \cdot Y + N_D \cdot \frac{S}{N_L} \cdot \frac{\partial Y}{\partial Z} = 0$$

Combining like terms results in:

$$-\frac{d \cdot S}{N_L} \cdot \frac{\partial^3 Y}{\partial Z^3} + \left(d + \frac{S}{N_L}\right) \cdot \frac{\partial^2 Y}{\partial Z^2} + \left(\frac{N_D \cdot S}{N_L} - 1 - S\right) \cdot \frac{\partial Y}{\partial Z} - N_D \cdot Y = 0$$

We now have a linear differential equation with constant coefficients.

Using a particular solution of $Y = EXP(\lambda Z)$, we get:

$$\left(-\frac{d \cdot S}{N_L}\right)\lambda^3 \cdot EXP(\lambda Z) + \left(d + \frac{S}{N_L}\right)\lambda^2 \cdot EXP(\lambda Z) + \left(\frac{N_D \cdot S}{N_L} - 1 - S\right)\lambda \cdot EXP(\lambda Z) - N_D \cdot EXP(\lambda Z) = 0$$

The general solution to this equation is:

$$Y = \alpha_1 \cdot EXP(\lambda_1 Z) + \alpha_2 \cdot EXP(\lambda_2 Z) + \alpha_3 \cdot EXP(\lambda_3 Z)$$

With this solution, we can develop expressions for $\frac{\partial Y}{\partial Z}, \frac{\partial^2 Y}{\partial Z^2}$ *and* $\frac{\partial^3 Y}{\partial Z^3}$ which will be useful later in the incorporation of boundary conditions.

$$\frac{\partial Y}{\partial Z} = \alpha_1 \cdot \lambda_1 \cdot EXP(\lambda_1 Z) + \alpha_2 \cdot \lambda_2 \cdot EXP(\lambda_2 Z) + \alpha_3 \cdot \lambda_3 \cdot EXP(\lambda_3 Z)$$

$$\frac{\partial^2 Y}{\partial Z^2} = \alpha_1 \cdot \lambda_1^2 \cdot EXP(\lambda_1 Z) + \alpha_2 \cdot \lambda_2^2 \cdot EXP(\lambda_2 Z) + \alpha_3 \cdot \lambda_3^2 \cdot EXP(\lambda_3 Z)$$

$$\frac{\partial^3 Y}{\partial Z^3} = \alpha_1 \cdot \lambda_1^3 \cdot EXP(\lambda_1 Z) + \alpha_2 \cdot \lambda_2^3 \cdot EXP(\lambda_2 Z) + \alpha_3 \cdot \lambda_3^3 \cdot EXP(\lambda_3 Z)$$

Now we can also develop expressions for $C_L, \frac{\partial C_L}{\partial Z}$ *and* $\frac{\partial^2 C_L}{\partial Z^2}$:

$$C_L = Y - \frac{S}{N_L}\frac{\partial Y}{\partial Z}$$

$$C_L = \left[EXP(\lambda_1 Z) - \frac{S}{N_L}\lambda_1 EXP(\lambda_1 Z)\right]\alpha_1 + \left[EXP(\lambda_2 Z) - \frac{S}{N_L}\lambda_2 EXP(\lambda_2 Z)\right]\alpha_2 + \left[EXP(\lambda_3 Z) - \frac{S}{N_L}\lambda_3 EXP(\lambda_3 Z)\right]\alpha_3$$

$$\frac{\partial C_L}{\partial Z} = \left[\lambda_1 EXP(\lambda_1 Z) - \frac{S}{N_L}\lambda_1^2 EXP(\lambda_1 Z)\right]\alpha_1 + \left[\lambda_2 EXP(\lambda_2 Z) - \frac{S}{N_L}\lambda_2^2 EXP(\lambda_2 Z)\right]\alpha_2 + \left[\lambda_3 EXP(\lambda_3 Z) - \frac{S}{N_L}\lambda_3^2 EXP(\lambda_3 Z)\right]\alpha_3$$

$$\frac{\partial^2 C_L}{\partial Z^2} = \left[\lambda_1^2 EXP(\lambda_1 Z) - \frac{S}{N_L}\lambda_1^3 EXP(\lambda_1 Z)\right]\alpha_1 + \left[\lambda_2^2 EXP(\lambda_2 Z) - \frac{S}{N_L}\lambda_2^3 EXP(\lambda_2 Z)\right]\alpha_2 + \left[\lambda_3^2 EXP(\lambda_3 Z) - \frac{S}{N_L}\lambda_3^3 EXP(\lambda_3 Z)\right]\alpha_3$$

We can now apply the first boundary condition:

$$C_L(Z=0) = d\frac{\partial C_L}{\partial Z}\Big|_{Z=0}$$

$$\left(1-\frac{S}{N_L}\lambda_1\right)\alpha_1+\left(1-\frac{S}{N_L}\lambda_2\right)\alpha_2+\left(1-\frac{S}{N_L}\lambda_3\right)\alpha_3=\left(d\lambda_1-\frac{dS}{N_L}\lambda_1^2\right)\alpha_1+\left(d\lambda_2-\frac{dS}{N_L}\lambda_2^2\right)\alpha_2+\left(d\lambda_3-\frac{dS}{N_L}\lambda_3^2\right)\alpha_3$$

Rearranging results in:

Equation 1:

$$\left(1-\frac{S}{N_L}\lambda_1-d\lambda_1+\frac{dS}{N_L}\lambda_1^2\right)\alpha_1+\left(1-\frac{S}{N_L}\lambda_2-d\lambda_2+\frac{dS}{N_L}\lambda_2^2\right)\alpha_2\left(1-\frac{S}{N_L}\lambda_3-d\lambda_3+\frac{dS}{N_L}\lambda_3^2\right)\alpha_3=0$$

The second boundary condition is:

$\frac{\partial C_L}{\partial Z}\Big|_{Z=1}=0$ resulting in:

Equation 2:

$$\left[\lambda_1 EXP(\lambda_1)-\frac{S}{N_L}\lambda_1^2 EXP(\lambda_1)\right]\alpha_1+\left[\lambda_2 EXP(\lambda_2)-\frac{S}{N_L}\lambda_2^2 EXP(\lambda_2)\right]\alpha_2+\left[\lambda_3 EXP(\lambda_3)-\frac{S}{N_L}\lambda_3^2 EXP(\lambda_3)\right]\alpha_3=0$$

For the third boundary condition, we need an expression for C_G in terms of C_L. From Equation I, we can solve for C_G as follows:

$$C_G=-\frac{d\cdot m}{N_L}\cdot\frac{\partial^2 C_L}{\partial Z^2}+\frac{m}{N_L}\cdot\frac{\partial C_L}{\partial Z}+\left(\frac{N_D\cdot m}{N_L}+m\right)\cdot C_L$$

Now we can apply the boundary condition : $C_G(Z=1)=C_{G,IN}$

$$-\frac{d\cdot m}{N_L}\left[\left(\lambda_1^2 EXP\ (\lambda_1)-\frac{s}{N_L}\lambda_1^3 EXP\ (\lambda_1)\right)\alpha_1+\left(\lambda_2^2 EXP\ (\lambda_2)-\frac{s}{N_L}\lambda_2^3 EXP\ (\lambda_2)\right)\alpha_2+\left(\lambda_3^2 EXP\ (\lambda_3)-\frac{s}{N_L}\lambda_3^3 EXP\ (\lambda_3)\right)\alpha_3\right]+$$

$$\frac{m}{N_L}\left[\left(\lambda_1 EXP\ (\lambda_1)-\frac{S}{N_L}\lambda_1^2 EXP\ (\lambda_1)\right)\alpha_1+\left(\lambda_2 EXP\ (\lambda_2)-\frac{S}{N_L}\lambda_2^2 EXP\ (\lambda_2)\right)\alpha_2+\left(\lambda_3 EXP\ (\lambda_3)-\frac{S}{N_L}\lambda_3^2 EXP\ (\lambda_3)\right)\alpha_3\right]+$$

$$\left(\frac{N_D m}{N_L}+m\right)\left[\left(EXP(\lambda_1)-\frac{S}{N_L}\lambda_1 EXP(\lambda_1)\right)\alpha_1+\left(EXP(\lambda_2)-\frac{S}{N_L}\lambda_2 EXP(\lambda_2)\right)\alpha_2+\left(EXP(\lambda_3)-\frac{S}{N_L}\lambda_3 EXP(\lambda_3)\right)\alpha_3\right]=C_{G,IN}$$

Combining like terms results in:

Equation 3:

$$\left[-\frac{d\cdot m}{N_L}\left(\lambda_1^2 EXP(\lambda_1)-\frac{S}{N_L}\lambda_1^3 EXP(\lambda_1)\right)+\frac{m}{N_L}\left(\lambda_1 EXP(\lambda_1)-\frac{S}{N_L}\lambda_1^2 EXP(\lambda_1)\right)+\left(\frac{N_D m}{N_L}+m\right)\left(EXP(\lambda_1)-\frac{S}{N_L}\lambda_1 EXP(\lambda_1)\right)\right]\alpha_1 +$$

$$\left[-\frac{d\cdot m}{N_L}\left(\lambda_2^2 EXP(\lambda_2)-\frac{S}{N_L}\lambda_2^3 EXP(\lambda_2)\right)+\frac{m}{N_L}\left(\lambda_2 EXP(\lambda_2)-\frac{S}{N_L}\lambda_2^2 EXP(\lambda_2)\right)+\left(\frac{N_D m}{N_L}+m\right)\left(EXP(\lambda_2)-\frac{S}{N_L}\lambda_2 EXP(\lambda_2)\right)\right]\alpha_2 +$$

$$\left[-\frac{d\cdot m}{N_L}\left(\lambda_3^2 EXP(\lambda_3)-\frac{S}{N_L}\lambda_3^3 EXP(\lambda_3)\right)+\frac{m}{N_L}\left(\lambda_3 EXP(\lambda_3)-\frac{S}{N_L}\lambda_3^2 EXP(\lambda_3)\right)+\left(\frac{N_D m}{N_L}+m\right)\left(EXP(\lambda_3)-\frac{S}{N_L}\lambda_3 EXP(\lambda_3)\right)\right]\alpha_3 = C_{G,IN}$$

We now have three equations with three unknowns: α_1, α_2 and α_3. (Once we solve for the roots λ_1, λ_2 and λ_3.)

Recalling that the roots can be determined from the linear differential equation:

$$\left(-\frac{d\cdot S}{N_L}\right)\cdot\lambda^3+\left(d+\frac{S}{N_L}\right)\cdot\lambda^2+\left(\frac{N_D\cdot S}{N_L}-1-S\right)\cdot\lambda-N_D=0$$

With the roots λ_1, λ_2 and λ_3, our three equations can be solved simultaneously for α_1, α_2 and α_3.

Recalling that $C_L = Y - \frac{S}{N_L}\cdot\frac{\partial Y}{\partial Z}$, we can solve for the concentration of dissolved ozone at any point in the contactor with the following equation:

$$C_L(Z)=\left(EXP(\lambda_1 Z)-\frac{S}{N_L}\lambda_1 EXP(\lambda_1 Z)\right)\alpha_1+\left(EXP(\lambda_2 Z)-\frac{S}{N_L}\lambda_2 EXP(\lambda_2 Z)\right)\alpha_2+\left(EXP(\lambda_3 Z)-\frac{S}{N_L}\lambda_3 EXP(\lambda_3 Z)\right)\alpha_3$$

Appendix III. Mass Balance for Co-Current Ozone Chamber

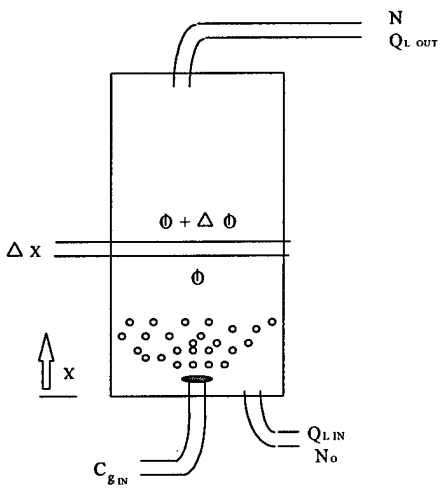

Liquid Side:

Mass Accumulation = Mass In – Mass Out + Mass Reacted + Mass Transferred

$$\Delta M = \Phi - (\Phi + \Delta\Phi) + V \cdot r_L + V \cdot r_C$$

$$\Delta M = C_L \cdot A \cdot \varepsilon \cdot \Delta X$$

$$\Phi = -E_L \cdot A \cdot \varepsilon \cdot \frac{\Delta C_L}{\Delta X} + Q_L \cdot C_L$$

$$r_L = K_{OL} \cdot a \cdot \varepsilon \cdot (C_L^* - C_L)$$

$$r_C = -K_D \cdot \varepsilon \cdot C_L$$

So the equation becomes:

$$\Delta(\Delta M) = -\Delta\Phi \cdot \Delta t + V \cdot r_L \cdot \Delta t + V \cdot r_C \cdot \Delta t$$

$$\Delta C_L A\varepsilon \cdot \Delta X = \left(E_L A\varepsilon \frac{\Delta^2 C_L}{\Delta X} - Q_L \Delta C_L \right) \Delta t + A\varepsilon \cdot \Delta X \cdot K_{OL} a (C_L^* - C_L) \Delta t - A\varepsilon \cdot \Delta X \cdot K_D C_L \Delta t$$

Dividing through by $A \cdot \varepsilon \cdot \Delta X \cdot \Delta t$ results in:

$$\frac{\Delta C_L}{\Delta t} = E_L \cdot \frac{\Delta^2 C_L}{\Delta X^2} - \frac{Q_L}{A \cdot \varepsilon} \cdot \frac{\Delta C_L}{\Delta X} + K_{OL} \cdot a \cdot \left(C_L^* - C_L\right) - K_D \cdot C_L$$

Taking the limit as the delta becomes infinitely small, $\Delta \to 0$, and additionally substituting K_L for K_{OL} since the mass transfer resistance on the gas side is negligible results in:

$$\frac{\partial C_L}{\partial t} = E_L \cdot \frac{\partial^2 C_L}{\partial X^2} - \frac{U_L}{\varepsilon} \cdot \frac{\partial C_L}{\partial X} + K_L \cdot a \cdot \left(C_L^* - C_L\right) - K_D \cdot C_L$$

To non-dimensionalize the equation, multiply each term by $\frac{L}{U_L}$:

$$\frac{L}{U_L} \cdot \frac{\partial C_L}{\partial t} = \frac{E_L \cdot L}{U_L} \cdot \frac{\partial^2 C_L}{\partial X^2} - \frac{U_L \cdot L}{\varepsilon \cdot U_L} \cdot \frac{\partial C_L}{\partial X} + \frac{K_L \cdot a \cdot L}{U_L} \cdot \left(C_L^* - C_L\right) - \frac{K_D \cdot L}{U_L} \cdot C_L$$

Non-dimensionalized coefficients will be defied as follows:

$$\Theta = \frac{t \cdot U_L}{L} \qquad N_L = \frac{K_L \cdot a \cdot L}{U_L}$$

$$Z = \frac{X}{L} \qquad N_D = \frac{K_D \cdot L}{U_L}$$

$$d = \frac{E_L}{U_L \cdot L} \qquad C_L^* = \frac{C_G}{m}$$

The non-dimensionalized equation then becomes:

$$\frac{\partial C_L}{\partial \Theta} = d \cdot \frac{\partial^2 C_L}{\partial Z^2} - \frac{1}{\varepsilon} \cdot \frac{\partial C_L}{\partial Z} + N_L \cdot \left(\frac{C_G}{m} - C_L\right) - N_D \cdot C_L$$

If the contactor is allowed to reach steady-state, then $\frac{\partial C_L}{\partial \Theta} = 0$ and:

The mass balance for the liquid side becomes:

$$d \cdot \frac{\partial^2 C_L}{\partial Z^2} - \frac{1}{\varepsilon} \cdot \frac{\partial C_L}{\partial Z} + N_L \cdot \left(\frac{C_G}{m} - C_L\right) - N_D \cdot C_L = 0$$

Gas Side:

Mass Accumulation = Mass In – Mass Out + Mass Reacted + Mass Transferred

$$\Delta M = C_G \cdot A \cdot (1-\varepsilon) \cdot \Delta X$$

$$\Phi = -E_G \cdot A \cdot (1-\varepsilon) \cdot \frac{\Delta C_G}{\Delta X} + Q_G \cdot C_G$$

$$r_L = K_L \cdot a \cdot \varepsilon \cdot (C_L^* - C_L)$$

$$r_C = -K_D \cdot (1-\varepsilon) \cdot C_L$$

So the equation becomes:

$$\Delta(\Delta M) = -\Delta\Phi \cdot \Delta t - V \cdot r_L \cdot \Delta t + V \cdot r_C \cdot \Delta t$$

$$\Delta C_G A(1-\varepsilon) \cdot \Delta X = \left(E_G A(1-\varepsilon) \frac{\Delta^2 C_G}{\Delta X} - Q_G \Delta C_G \right) \Delta t - A(1-\varepsilon) \cdot \Delta X \cdot K_L a (C_L^* - C_L) \Delta t - A(1-\varepsilon) \cdot \Delta X \cdot K_D C_G \Delta t$$

Dividing through by $A \cdot (1-\varepsilon) \cdot \Delta X \cdot \Delta t$ results in:

$$\frac{\Delta C_G}{\Delta t} = E_G \cdot \frac{\Delta^2 C_G}{\Delta X^2} - \frac{Q_G}{A \cdot (1-\varepsilon)} \cdot \frac{\Delta C_G}{\Delta X} - \frac{\varepsilon}{(1-\varepsilon)} K_L \cdot a \cdot (C_L^* - C_L) - K_D \cdot C_G$$

Taking the limit as the delta becomes infinitely small, $\Delta \to 0$ results in:

$$\frac{\partial C_G}{\partial t} = E_G \cdot \frac{\partial^2 C_G}{\partial X^2} - \frac{U_G}{1-\varepsilon} \cdot \frac{\partial C_G}{\partial X} - \frac{\varepsilon}{(1-\varepsilon)} \cdot K_L \cdot a \cdot (C_L^* - C_L) - K_D \cdot C_G$$

To non-dimensionalize the equation, multiply each term by $\frac{L}{U_L}$:

$$\frac{L}{U_L} \cdot \frac{\partial C_G}{\partial t} = \frac{E_G \cdot L}{U_L} \cdot \frac{\partial^2 C_G}{\partial X^2} - \frac{U_G \cdot L}{(1-\varepsilon) \cdot U_L} \cdot \frac{\partial C_G}{\partial X} - \frac{K_L \cdot a \cdot L \cdot \varepsilon}{(1-\varepsilon) \cdot U_L} \cdot (C_L^* - C_L) - \frac{K_D \cdot L}{U_L} \cdot C_G$$

The non-dimensionalized equation then becomes:

$$\frac{\partial C_G}{\partial \Theta} = \frac{E_G}{U_L \cdot L} \cdot \frac{\partial^2 C_G}{\partial Z^2} - \frac{U_G}{U_L \cdot (1-\varepsilon)} \cdot \frac{\partial C_G}{\partial Z} - \frac{N_L \cdot \varepsilon}{(1-\varepsilon)} \cdot (C_L^* - C_L) - N_D \cdot C_G$$

If the contactor is allowed to reach steady-state, then $\frac{\partial C_G}{\partial \Theta} = 0$.

Additionally, considering that diffusivity in the gas bubbles is extremely small and ozone is non-reactive in air, we can eliminate two additional terms.

The mass balance for the gas side becomes:

$$-\frac{U_G}{U_L \cdot (1-\varepsilon)} \cdot \frac{\partial C_G}{\partial Z} - \frac{N_L \cdot \varepsilon}{(1-\varepsilon)} \cdot \left(C_L^* - C_L\right) = 0$$

Since $C_L^* = \frac{C_G}{m}$, and $S = \frac{m \cdot U_G}{U_L}$, the equation becomes,

$$\frac{S}{(1-\varepsilon)} \cdot \frac{\partial\left(\frac{C_G}{m}\right)}{\partial Z} + \frac{\varepsilon}{(1-\varepsilon)} \cdot N_L \cdot \left(\frac{C_G}{m} - C_L\right) = 0$$

Now we have two equations representing our system. Assuming $\varepsilon \cong 1$ for ozone, the two equations reduce to the final form:

I. $$d\frac{\partial^2 C_L}{\partial Z^2} - \frac{\partial C_L}{\partial Z} + N_L \cdot \left(\frac{C_G}{m} - C_L\right) - N_D \cdot C_L = 0$$

II. $$\frac{\partial\left(\frac{C_G}{m}\right)}{\partial Z} + \frac{N_L}{S}\left(\frac{C_G}{m} - C_L\right) = 0$$

Using the boundary conditions:

Liquid:

$$C_L(Z=0) = C_{L,IN} + d\frac{\partial C_L}{\partial Z}\Big|_{Z=0} \quad \text{(Inlet)}$$

$$\frac{\partial C_L}{\partial Z}\Big|_{Z=1} = 0 \quad \text{(Outlet)}$$

Gas:

$$C_G(Z=0) = C_{G,IN}$$

If in Equation II, we let $Y = \frac{C_G}{m}$, we get:

$$\frac{\partial Y}{\partial Z} + \frac{N_L}{S}(Y - C_L) = 0$$

We can rearrange and solve for C_L in terms of Y as follows:

$$C_L = Y + \frac{S}{N_L} \cdot \frac{\partial Y}{\partial Z}$$

With an expression for C_L in terms of Y, we can develop expressions for the first and second derivatives of C_L as follows:

$$\frac{\partial C_L}{\partial Z} = \frac{\partial Y}{\partial Z} + \frac{S}{N_L} \cdot \frac{\partial^2 Y}{\partial Z^2} \qquad \text{and}$$

$$\frac{\partial^2 C_L}{\partial Z^2} = \frac{\partial^2 Y}{\partial Z^2} + \frac{S}{N_L} \cdot \frac{\partial^3 Y}{\partial Z^3}$$

Substitution into Equation I results in:

$$d\left(\frac{\partial^2 Y}{\partial Z^2} + \frac{S}{N_L} \cdot \frac{\partial^3 Y}{\partial Z^3}\right) - \left(\frac{\partial Y}{\partial Z} + \frac{S}{N_L} \cdot \frac{\partial^2 Y}{\partial Z^2}\right) + N_L\left[Y - \left(Y + \frac{S}{N_L} \cdot \frac{\partial Y}{\partial Z}\right)\right] - N_D\left(Y + \frac{S}{N_L} \cdot \frac{\partial Y}{\partial Z}\right) = 0$$

or

$$d\frac{\partial^2 Y}{\partial Z^2} + d \cdot \frac{S}{N_L} \cdot \frac{\partial^3 Y}{\partial Z^3} - \frac{\partial Y}{\partial Z} - \frac{S}{N_L} \cdot \frac{\partial^2 Y}{\partial Z^2} - S \cdot \frac{\partial Y}{\partial Z} - N_D \cdot Y - N_D \cdot \frac{S}{N_L} \cdot \frac{\partial Y}{\partial Z} = 0$$

Combining like terms results in:

$$\frac{d \cdot S}{N_L} \cdot \frac{\partial^3 Y}{\partial Z^3} + \left(d - \frac{S}{N_L}\right) \cdot \frac{\partial^2 Y}{\partial Z^2} - \left(1 + S + \frac{N_D \cdot S}{N_L}\right) \cdot \frac{\partial Y}{\partial Z} - N_D \cdot Y = 0$$

We now have a linear differential equation with constant coefficients.

Using a particular solution of $Y = EXP(\lambda Z)$, we get:

$$\left(\frac{d \cdot S}{N_L}\right)\lambda^3 \cdot EXP(\lambda Z) + \left(d - \frac{S}{N_L}\right)\lambda^2 \cdot EXP(\lambda Z) - \left(1 + S + \frac{N_D \cdot S}{N_L}\right)\lambda \cdot EXP(\lambda Z) - N_D \cdot EXP(\lambda Z) = 0$$

The general solution to this equation is:

$$Y = \alpha_1 \cdot EXP(\lambda_1 Z) + \alpha_2 \cdot EXP(\lambda_2 Z) + \alpha_3 \cdot EXP(\lambda_3 Z)$$

With this solution, we can develop expressions for $\frac{\partial Y}{\partial Z}, \frac{\partial^2 Y}{\partial Z^2}$ *and* $\frac{\partial^3 Y}{\partial Z^3}$ which will be useful later in the incorporation of boundary conditions.

$$\frac{\partial Y}{\partial Z} = \alpha_1 \cdot \lambda_1 \cdot EXP(\lambda_1 Z) + \alpha_2 \cdot \lambda_2 \cdot EXP(\lambda_2 Z) + \alpha_3 \cdot \lambda_3 \cdot EXP(\lambda_3 Z)$$

$$\frac{\partial^2 Y}{\partial Z^2} = \alpha_1 \cdot \lambda_1^2 \cdot EXP(\lambda_1 Z) + \alpha_2 \cdot \lambda_2^2 \cdot EXP(\lambda_2 Z) + \alpha_3 \cdot \lambda_3^2 \cdot EXP(\lambda_3 Z)$$

$$\frac{\partial^3 Y}{\partial Z^3} = \alpha_1 \cdot \lambda_1^3 \cdot EXP(\lambda_1 Z) + \alpha_2 \cdot \lambda_2^3 \cdot EXP(\lambda_2 Z) + \alpha_3 \cdot \lambda_3^3 \cdot EXP(\lambda_3 Z)$$

Now we can also develop expressions for $C_L, \frac{\partial C_L}{\partial Z}$ *and* $\frac{\partial^2 C_L}{\partial Z^2}$:

$$C_L = Y + \frac{S}{N_L}\frac{\partial Y}{\partial Z}$$

$$C_L = \left[EXP(\lambda_1 Z) + \frac{S}{N_L}\lambda_1 EXP(\lambda_1 Z)\right]\alpha_1 + \left[EXP(\lambda_2 Z) + \frac{S}{N_L}\lambda_2 EXP(\lambda_2 Z)\right]\alpha_2 + \left[EXP(\lambda_3 Z) + \frac{S}{N_L}\lambda_3 EXP(\lambda_3 Z)\right]\alpha_3$$

$$\frac{\partial C_L}{\partial Z} = \left[\lambda_1 EXP(\lambda_1 Z) + \frac{S}{N_L}\lambda_1^2 EXP(\lambda_1 Z)\right]\alpha_1 + \left[\lambda_2 EXP(\lambda_2 Z) + \frac{S}{N_L}\lambda_2^2 EXP(\lambda_2 Z)\right]\alpha_2 + \left[\lambda_3 EXP(\lambda_3 Z) + \frac{S}{N_L}\lambda_3^2 EXP(\lambda_3 Z)\right]\alpha_3$$

$$\frac{\partial^2 C_L}{\partial Z^2} = \left[\lambda_1^2 EXP(\lambda_1 Z) + \frac{S}{N_L}\lambda_1^3 EXP(\lambda_1 Z)\right]\alpha_1 + \left[\lambda_2^2 EXP(\lambda_2 Z) + \frac{S}{N_L}\lambda_2^3 EXP(\lambda_2 Z)\right]\alpha_2 + \left[\lambda_3^2 EXP(\lambda_3 Z) + \frac{S}{N_L}\lambda_3^3 EXP(\lambda_3 Z)\right]\alpha_3$$

We can now apply the first boundary condition:

$$C_L(Z=0) = d\frac{\partial C_L}{\partial Z}\Big|_{Z=0}$$

$$\left(1+\frac{S}{N_L}\lambda_1\right)\alpha_1+\left(1+\frac{S}{N_L}\lambda_2\right)\alpha_2+\left(1+\frac{S}{N_L}\lambda_3\right)\alpha_3=\left(d\lambda_1+\frac{dS}{N_L}\lambda_1^2\right)\alpha_1+\left(d\lambda_2+\frac{dS}{N_L}\lambda_2^2\right)\alpha_2+\left(d\lambda_3+\frac{dS}{N_L}\lambda_3^2\right)\alpha_3$$

Rearranging results in:

Equation 1:

$$\left(1+\frac{S}{N_L}\lambda_1-d\lambda_1-\frac{dS}{N_L}\lambda_1^2\right)\alpha_1+\left(1+\frac{S}{N_L}\lambda_2-d\lambda_2-\frac{dS}{N_L}\lambda_2^2\right)\alpha_2\left(1+\frac{S}{N_L}\lambda_3-d\lambda_3-\frac{dS}{N_L}\lambda_3^2\right)\alpha_3=0$$

The second boundary condition is:

$\frac{\partial C_L}{\partial Z}\Big|_{Z=1}=0$ resulting in:

Equation 2:

$$\left[\lambda_1 EXP(\lambda_1)+\frac{S}{N_L}\lambda_1^2 EXP(\lambda_1)\right]\alpha_1+\left[\lambda_2 EXP(\lambda_2)+\frac{S}{N_L}\lambda_2^2 EXP(\lambda_2)\right]\alpha_2+\left[\lambda_3 EXP(\lambda_3)+\frac{S}{N_L}\lambda_3^2 EXP(\lambda_3)\right]\alpha_3=0$$

For the third boundary condition, we need an expression for C_G in terms of C_L. From Equation I, we can solve for C_G as follows:

$$C_G=-\frac{d\cdot m}{N_L}\cdot\frac{\partial^2 C_L}{\partial Z^2}+\frac{m}{N_L}\cdot\frac{\partial C_L}{\partial Z}+\left(\frac{N_D\cdot m}{N_L}+m\right)\cdot C_L$$

Now we can apply the boundary condition : $C_G(Z=0)=C_{G,IN}$

$$-\frac{d\cdot m}{N_L}\left[\left(\lambda_1^2 EXP(\lambda_1)+\frac{s}{N_L}\lambda_1^3 EXP(\lambda_1)\right)\alpha_1+\left(\lambda_2^2 EXP(\lambda_2)+\frac{s}{N_L}\lambda_2^3 EXP(\lambda_2)\right)\alpha_2+\left(\lambda_3^2 EXP(\lambda_3)+\frac{s}{N_L}\lambda_3^3 EXP(\lambda_3)\right)\alpha_3\right]+$$

$$\frac{m}{N_L}\left[\left(\lambda_1 EXP(\lambda_1)+\frac{S}{N_L}\lambda_1^2 EXP(\lambda_1)\right)\alpha_1+\left(\lambda_2 EXP(\lambda_2)+\frac{S}{N_L}\lambda_2^2 EXP(\lambda_2)\right)\alpha_2+\left(\lambda_3 EXP(\lambda_3)+\frac{S}{N_L}\lambda_3^2 EXP(\lambda_3)\right)\alpha_3\right]+$$

$$\left(\frac{N_D m}{N_L}+m\right)\left[\left(EXP(\lambda_1)+\frac{S}{N_L}\lambda_1 EXP(\lambda_1)\right)\alpha_1+\left(EXP(\lambda_2)+\frac{S}{N_L}\lambda_2 EXP(\lambda_2)\right)\alpha_2+\left(EXP(\lambda_3)+\frac{S}{N_L}\lambda_3 EXP(\lambda_3)\right)\alpha_3\right]=C_{G,IN}$$

Combining like terms results in:

Equation 3:

$$\left[-\frac{d\cdot m}{N_L}\left(\lambda_1^2 EXP(\lambda_1)+\frac{S}{N_L}\lambda_1^3 EXP(\lambda_1)\right)+\frac{m}{N_L}\left(\lambda_1 EXP(\lambda_1)+\frac{S}{N_L}\lambda_1^2 EXP(\lambda_1)\right)+\left(\frac{N_D m}{N_L}+m\right)\left(EXP(\lambda_1)+\frac{S}{N_L}\lambda_1 EXP(\lambda_1)\right)\right]\alpha_1 +$$

$$\left[-\frac{d\cdot m}{N_L}\left(\lambda_2^2 EXP(\lambda_2)+\frac{S}{N_L}\lambda_2^3 EXP(\lambda_2)\right)+\frac{m}{N_L}\left(\lambda_2 EXP(\lambda_2)+\frac{S}{N_L}\lambda_2^2 EXP(\lambda_2)\right)+\left(\frac{N_D m}{N_L}+m\right)\left(EXP(\lambda_2)+\frac{S}{N_L}\lambda_2 EXP(\lambda_2)\right)\right]\alpha_2 +$$

$$\left[-\frac{d\cdot m}{N_L}\left(\lambda_3^2 EXP(\lambda_3)+\frac{S}{N_L}\lambda_3^3 EXP(\lambda_3)\right)+\frac{m}{N_L}\left(\lambda_3 EXP(\lambda_3)+\frac{S}{N_L}\lambda_3^2 EXP(\lambda_3)\right)+\left(\frac{N_D m}{N_L}+m\right)\left(EXP(\lambda_3)+\frac{S}{N_L}\lambda_3 EXP(\lambda_3)\right)\right]\alpha_3 = C_{G,IN}$$

We now have three equations with three unknowns: α_1, α_2 and α_3. (Once we solve for the roots λ_1, λ_2 and λ_3.)

Recalling that the roots can be determined from the linear differential equation:

$$\left(\frac{d\cdot S}{N_L}\right)\cdot\lambda^3+\left(d-\frac{S}{N_L}\right)\cdot\lambda^2-\left(1+S+\frac{N_D\cdot S}{N_L}\right)\cdot\lambda-N_D=0$$

With the roots λ_1, λ_2 and λ_3, our three equations can be solved simultaneously for α_1, α_2 and α_3.

Recalling that $C_L = Y + \frac{S}{N_L}\cdot\frac{\partial Y}{\partial Z}$, we can solve for the concentration of dissolved ozone at any point in the contactor with the following equation:

$$C_L(Z)=\left(EXP(\lambda_1 Z)+\frac{S}{N_L}\lambda_1 EXP(\lambda_1 Z)\right)\alpha_1+\left(EXP(\lambda_2 Z)+\frac{S}{N_L}\lambda_2 EXP(\lambda_2 Z)\right)\alpha_2+\left(EXP(\lambda_3 Z)+\frac{S}{N_L}\lambda_3 EXP(\lambda_3 Z)\right)\alpha_3$$

Appendix IV. Mass Balance for Reactive Ozone Chamber

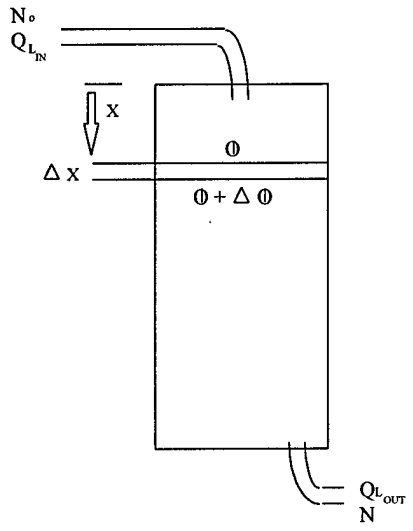

Mass Accumulation = Mass In – Mass Out + Mass Reacted + Mass Transferred

$$\Delta M = \Phi - (\Phi + \Delta\Phi) + V \cdot r_L + V \cdot r_C$$

$$\Delta M = C_L \cdot A \cdot \varepsilon \cdot \Delta X$$

$$\Phi = -E_L \cdot A \cdot \varepsilon \cdot \frac{\Delta C_L}{\Delta X} + Q_L \cdot C_L$$

$r_L = 0$ (No ozone vapor bubbles)

$$r_C = -K_D \cdot \varepsilon \cdot C_L$$

So the equation becomes:

$$\Delta(\Delta M) = -\Delta\Phi \cdot \Delta t + V \cdot r_C \cdot \Delta t$$

$$\Delta C_L A\varepsilon \cdot \Delta X = \left(E_L A\varepsilon \frac{\Delta^2 C_L}{\Delta X} - Q_L \Delta C_L \right) \Delta t - A\varepsilon \cdot \Delta X \cdot K_D C_L \Delta t$$

Dividing through by $A \cdot \varepsilon \cdot \Delta X \cdot \Delta t$ results in:

$$\frac{\Delta C_L}{\Delta t} = E_L \cdot \frac{\Delta^2 C_L}{\Delta X^2} - \frac{Q_L}{A \cdot \varepsilon} \cdot \frac{\Delta C_L}{\Delta X} - K_D \cdot C_L$$

Taking the limit as the delta becomes infinitely small, $\Delta \to 0$, and additionally substituting K_L for K_{OL} since the mass transfer resistance on the gas side is negligible results in:

$$\frac{\partial C_L}{\partial t} = E_L \cdot \frac{\partial^2 C_L}{\partial X^2} - \frac{U_L}{\varepsilon} \cdot \frac{\partial C_L}{\partial X} - K_D \cdot C_L$$

To non-dimensionalize the equation, multiply each term by $\frac{L}{U_L}$:

$$\frac{L}{U_L} \cdot \frac{\partial C_L}{\partial t} = \frac{E_L \cdot L}{U_L} \cdot \frac{\partial^2 C_L}{\partial X^2} - \frac{U_L \cdot L}{\varepsilon \cdot U_L} \cdot \frac{\partial C_L}{\partial X} - \frac{K_D \cdot L}{U_L} \cdot C_L$$

Non-dimensionalized coefficients will be defied as follows:

$$\Theta = \frac{t \cdot U_L}{L}$$

$$Z = \frac{X}{L} \qquad N_D = \frac{K_D \cdot L}{U_L}$$

$$d = \frac{E_L}{U_L \cdot L}$$

The non-dimensionalized equation then becomes:

$$\frac{\partial C_L}{\partial \Theta} = d \cdot \frac{\partial^2 C_L}{\partial Z^2} - \frac{1}{\varepsilon} \cdot \frac{\partial C_L}{\partial Z} - N_D \cdot C_L$$

If the contactor is allowed to reach steady-state, then $\frac{\partial C_L}{\partial \Theta} = 0$ and:

The mass balance for the liquid side becomes:

$$d \cdot \frac{\partial^2 C_L}{\partial Z^2} - \frac{1}{\varepsilon} \cdot \frac{\partial C_L}{\partial Z} - N_D \cdot C_L = 0$$

Again, assuming $\varepsilon \cong 1$ for ozone, the equation reduces to the final form:

$$d\frac{\partial^2 C_L}{\partial Z^2} - \frac{\partial C_L}{\partial Z} - N_D \cdot C_L = 0$$

If we let $Y=C_L$, we get:

$$d\frac{\partial^2 Y}{\partial Z^2} - \frac{\partial Y}{\partial Z} - N_D Y = 0$$

We again have a linear differential equation with constant coefficients. Using a particular solution of $Y = EXP(\lambda \cdot Z)$, we get:

$$d \cdot \lambda^2 EXP(\lambda \cdot Z) - \lambda EXP(\lambda \cdot Z) - N_D EXP(\lambda \cdot Z) = 0$$

After dividing through by $EXP(\lambda \cdot Z)$, we get:

$$d \cdot \lambda^2 - \lambda - N_D = 0$$

The general solution to this equation is:

$$C_L = Y = \beta_1 \cdot EXP(\lambda_4 \cdot Z) + \beta_2 \cdot EXP(\lambda_5 \cdot Z)$$

We can now develop an expression for $\frac{\partial Y}{\partial Z}$ which will be useful later in the evaluation of boundary conditions:

$$\frac{\partial C_L}{\partial Z} = \frac{\partial Y}{\partial Z} = \beta_1 \cdot \lambda_4 \cdot EXP(\lambda_4 \cdot Z) + \beta_2 \cdot \lambda_5 \cdot EXP(\lambda_5 \cdot Z)$$

Our first boundary condition is that the input to the reactive chamber is the output of the previous chamber:

$C_L(Z=0) = C_{L,OUT}^{PreviousChamber}$ (Inlet) Since C_L=Y, we get:

Equation 1: $\beta_1 + \beta_2 = C_{L,OUT}^{PreviousChamber}$

The second boundary condition is:

$\frac{\partial C_L}{\partial Z}\Big|_{Z=1} = 0$, (Outlet) resulting in:

Equation 2: $[\lambda_4 \cdot EXP(\lambda_4)]\beta_1 + [\lambda_5 \cdot EXP(\lambda_5)]\beta_2 = 0$

We now have two equations with two unknowns: β_1 and β_2. (Once we solve for the roots λ_4 and λ_5.)

Recalling that the roots can be determined from the linear differential equation:

$$d \cdot \lambda^2 - \lambda - N_D = 0$$

With the roots λ_4 and λ_5, our two equations can be solved simultaneously for β_1 and β_2.

We can now solve for the concentration of dissolved ozone at any point in the reactive chamber:

$$C_L(Z) = \beta_1 \cdot EXP(\lambda_4 \cdot Z) + \beta_2 \cdot EXP(\lambda_5 \cdot Z)$$

Since no gas bubbles are applied in a reactive chamber, it may be assumed that turbulent dispersivity is minimal and approaches "plug flow" conditions. Thus, the dispersion term may be ommited and our equations simplified.

The mass balance for the liquid side becomes:

$$\frac{\partial C_L}{\partial Z} + N_D \cdot C_L = 0$$

Using a particular solution of:

$$C_L = Y = EXP(\lambda \cdot Z)$$

We get the following equation:

$$\lambda \cdot EXP(\lambda \cdot Z) + N_D \cdot EXP(\lambda \cdot Z) = 0$$

Solving, we find that the root (λ) = -N_D.

The general solution to this equation is then:

$$C_L = Y = \alpha \cdot EXP(-N_D \cdot Z)$$

Only one boundary condition is required. The input to the reactive chamber is the output of the previous chamber:

$$C_L(Z=0) = C_{L,OUT}^{PreviousChamber} \quad \text{(Inlet)}$$

This allows for the development of an equation representing the concentration of dissolved ozone at any point in the reactive chamber when dispersion is assumed to be negligible:

$$C_L(Z) = C_{L,OUT}^{PreviousChamber} \cdot EXP(-N_D \cdot Z)$$

Appendix V. Mass Balance for Cryptosporidium Inactivation

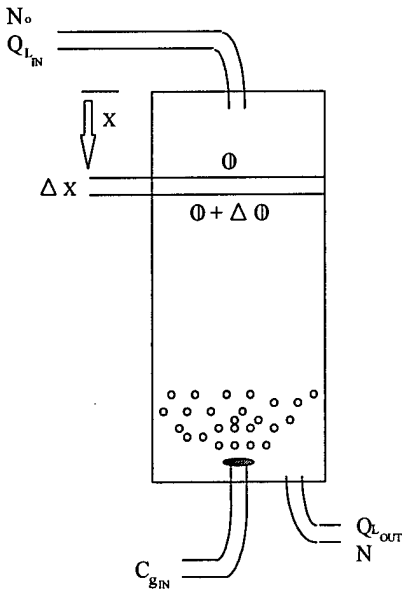

Mass Accumulation = Mass In – Mass Out + Mass Reacted

$$\Delta M = \Phi - (\Phi + \Delta\Phi) + V \cdot r_N$$

$$\Delta M = N \cdot A \cdot \Delta X \quad \text{(Where N = Quantity of active oocysts)}$$

$$\Phi = -E_L \cdot A \cdot \frac{\Delta N}{\Delta X} + Q_L \cdot N$$

$$r_C = -K_N \cdot N \cdot C_L$$

So the equation becomes:

$$\Delta(\Delta M) = -\Delta\Phi \cdot \Delta t + V \cdot r_N \cdot \Delta t$$

$$\Delta N \cdot A \cdot \Delta X = \left(E_L A \frac{\Delta^2 N}{\Delta X} - Q_L \Delta N \right) \Delta t - A \cdot \Delta X \cdot K_N \cdot N \cdot C_L \Delta t$$

Dividing through by $A \cdot \Delta X \cdot \Delta t$ results in:

$$\frac{\Delta N}{\Delta t} = E_L \cdot \frac{\Delta^2 N}{\Delta X^2} - \frac{Q_L}{A} \cdot \frac{\Delta N}{\Delta X} - K_N \cdot N \cdot C_L$$

Taking the limit as the delta becomes infinitely small, $\Delta \to 0$, results in:

$$\frac{\partial N}{\partial t} = E_L \cdot \frac{\partial^2 N}{\partial X^2} - U_L \cdot \frac{\partial N}{\partial X} - K_N \cdot N \cdot C_L$$

To non-dimensionalize the equation, multiply each term by $\frac{L}{U_L}$:

$$\frac{L}{U_L} \cdot \frac{\partial N}{\partial t} = \frac{E_L \cdot L}{U_L} \cdot \frac{\partial^2 N}{\partial X^2} - \frac{U_L \cdot L}{U_L} \cdot \frac{\partial N}{\partial X} - \frac{K_N \cdot N \cdot L}{U_L} \cdot C_L$$

Non-dimensionalized coefficients will be defied as follows:

$$\Theta = \frac{t \cdot U_L}{L} \qquad d = \frac{E_L}{U_L \cdot L}$$

$$Z = \frac{X}{L} \qquad N_N = \frac{K_N \cdot L}{U_L}$$

The non-dimensionalized equation then becomes:

$$\frac{\partial N}{\partial \Theta} = d \cdot \frac{\partial^2 N}{\partial Z^2} - \frac{\partial N}{\partial Z} - N_N \cdot N \cdot C_L$$

If the contactor is allowed to reach steady-state, then $\frac{\partial N}{\partial \Theta} = 0$ and in final form, we have:

$$d \cdot \frac{\partial^2 N}{\partial Z^2} - \frac{\partial N}{\partial Z} - N_N \cdot N \cdot C_L = 0$$

Our boundary conditions are:

$N(Z=0) = N_0 + d \left. \frac{\partial N}{\partial Z} \right|_{z=0}$ (Inlet) and

$\left. \frac{\partial N}{\partial Z} \right|_{Z=1} = 0$ (Outlet)

Using a finite difference approach, we can develop a profile for *Cryptosporidium* inactivation through the contactor.

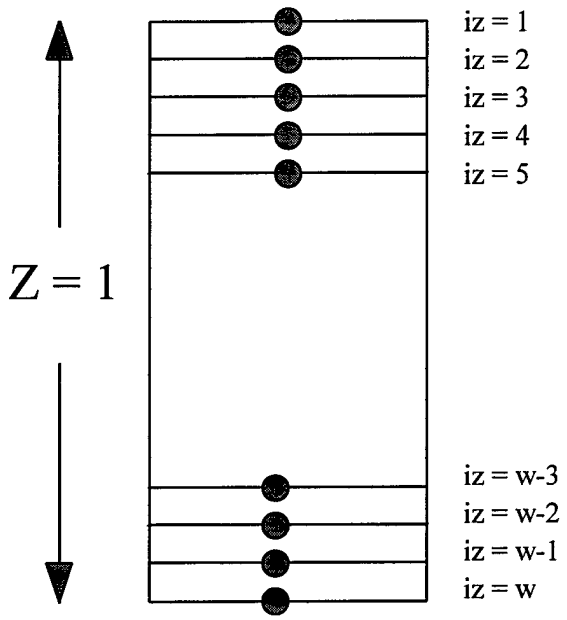

$iz = 1 \longrightarrow w$

Space increment $\Delta z = \frac{1}{w\text{-}1}$

If we let $w = 401$, $\Delta z = 0.0025$

The expression for $\frac{\partial N}{\partial Z}\Big|_{iz} = \frac{N(iz+1) - N(iz-1)}{2\Delta Z}$

At the top of the contactor (where $iz = 1$), we have:

$$\frac{\partial N}{\partial Z}\Big|_{iz=1} = \frac{-N(iz+2) + 4N(iz+1) - 3N(iz)}{2\Delta Z}$$

At the bottom of the contactor (where $iz = w$), we have:

$$\frac{\partial N}{\partial Z}\Big|_{iz=w} = \frac{N(iz-2) - 4N(iz-1) + 3N(iz)}{2\Delta Z}$$

Ou expression for every increment in between is:

$$\frac{\partial^2 N}{\partial Z^2}\Big|_{iz} = \frac{N(iz+1) - 2N(iz) + N(iz-1)}{(\Delta Z)^2}$$

At $iz = 1$ and $iz = w$, we can apply our boundary conditions:

At iz = 1:

$$N(1)-d\left[\frac{-N(3)+4N(2)-3N(1)}{2\Delta Z}\right]=N_o$$

At iz = w:

$$\frac{N(w-2)-4N(w-1)+3N(w)}{2\Delta Z}=0$$

By rearranging , the first equation becomes:

$$N(1)+\frac{d}{2\Delta Z}N(3)-\frac{4d}{2\Delta Z}N(2)+\frac{3d}{2\Delta Z}N(1)=N_o$$

After grouping like terms, the first equation becomes:

1) $$\underbrace{\left(1+\frac{3d}{2\Delta Z}\right)}_{\text{B(1)}}N(1)\underbrace{-\frac{2d}{\Delta Z}}_{\text{D(1)}}N(2)\underbrace{+\frac{d}{2\Delta Z}}_{\text{X(1)}}N(3)\underbrace{=N_o}_{\text{G(1)}}$$

Similarly, the second equation becomes:

2) $$\underbrace{\frac{1}{2\Delta Z}}_{\text{X(w)}}N(w-2)\underbrace{-\frac{2}{\Delta Z}}_{\text{A(w)}}N(w-1)\underbrace{+\frac{3}{2\Delta Z}}_{\text{B(w)}}N(w)\underbrace{=0}_{\text{G(w)}}$$

Between the boundary conditions, we have for 1<iz<w:

$$d\left[\frac{N(iz+1)-2N(iz)+N(iz-1)}{\Delta Z^2}\right]-\left[\frac{N(iz+1)-N(iz-1)}{2\Delta Z}\right]-N_N C_L(iz)N(iz)=0$$

Rearranging, we have:

$$\frac{d}{\Delta Z^2}N(iz+1)-\frac{2d}{\Delta Z^2}N(iz)+\frac{d}{\Delta Z^2}N(iz-1)-\frac{1}{2\Delta Z}N(iz+1)+\frac{1}{2\Delta Z}N(iz-1)-N_N C_L(iz)N(iz)=0$$

Grouping like terms results in:

3) $$\underbrace{\left[\frac{d}{\Delta Z^2}+\frac{1}{2\Delta Z}\right]}_{A(iz)}N(iz-1)+\underbrace{\left[-\frac{2d}{\Delta Z^2}-N_d C_L(iz)\right]}_{B(iz)}N(iz)+\underbrace{\left[\frac{d}{\Delta Z^2}-\frac{1}{2\Delta Z}\right]}_{D(iz)}N(iz+1)=\underbrace{0}_{G(iz)}$$

We then have the following equations:

For iz =

iz = 1	B(1) N(1) + D(1) N(2) + X(1) N(3) = G(1)
iz = 2	A(2) N(1) + B(2) N(2) + D(2) N(3) = G(2)
iz = 3	A(3) N(2) + B(3) N(3) + D(3) N(4) = G(3)
iz = 4	A(4) N(3) + B(4) N(4) + D(4) N(5) = G(4)
⇓	⇓
⇓	⇓
⇓	⇓
iz=w-3	A(w-3) N(w-4) + B(w-3) N(w-3) + D(w-3) N(w-2) = G(w-3)
iz=w-2	A(w-2) N(w-3) + B(w-2) N(w-2) + D(w-2) N(w-1) = G(w-2)
iz=w-1	A(w-1) N(w-2) + B(w-1) N(w-1) + D(w-1) N(w) = G(w-1)
iz=w	X(w) N(w-2) + A(w) N(w-1) + B(w) N(w) = G(w)

We can then represent these equations by a matrix:

B(1)	D(1)	X(1)	0	0	⇒	⇒
A(2)	B(2)	D(2)	0	0	⇒	⇒
0	A(3)	B(3)	D(3)	0	⇒	⇒
0	0	A(4)	B(4)	D(4)	⇒	⇒
⇓	⇓	⇓	⇓	⇓		
⇓	⇓	⇓	⇓	⇓		

D(w-3)	0	0
B(w-2)	D(w-2)	0
A(w-1)	B(w-1)	D(w-1)
X(w)	A(w)	B(w)

The tri-diagonal matrix is represented as follows:

$$\begin{bmatrix} N(1) \\ N(2) \\ N(3) \\ \Downarrow \\ \Downarrow \\ N(w-2) \\ N(w-1) \\ N(w) \end{bmatrix} \text{x} \begin{bmatrix} B(1)N(1)+D(1)N(1)+X(1)N(1) \\ A(2)N(2)+B(2)N(2)+D(2)N(2) \\ A(3)N(3)+B(3)N(3)+D(3)N(3) \\ \Downarrow \\ \Downarrow \\ A(w-2)N(w-2)+B(w-2)N(w-2)+D(w-2N(w-2) \\ A(w-1)N(w-1)+B(w-1)N(w-1)+D(w-1)N(w-1) \\ X(w)N(w)+A(w)N(w)+B(w)N(w) \end{bmatrix} = \begin{bmatrix} G(1) \\ G(2) \\ G(3) \\ \Downarrow \\ \Downarrow \\ G(w-2) \\ G(w-1) \\ G(w) \end{bmatrix}$$

The Thomas Method may now be employed to solve the tri-diagonal matrix:

$$\text{N(1)} = \underbrace{\frac{\frac{G(1)}{B(1)} - \frac{X(1)G(2)}{B(1)D(2)}}{1-\frac{X(1)A(2)}{B(1)D(2)}}}_{\text{ETA(1)}} - \underbrace{\frac{\frac{D(1)}{B(1)} - \frac{X(1)B(2)}{B(1)D(2)}}{1-\frac{X(1)A(2)}{B(1)D(2)}}}_{\text{E(1)}} \text{N(2)}$$

or

$$\text{N(1)} = \text{ETA(1)} - \text{E(1)N(2)}$$

Substitution into the second matrix equation results in:

$$\text{N(2)} = \underbrace{\frac{G(2)-A(2)ETA(1)}{B(2)-A(2)E(1)}}_{\text{ETA(2)}} - \underbrace{\frac{D(2)}{B(2)-A(2)E(1)}}_{\text{E(2)}} \text{N(3)}$$

or

$$\text{N(2)} = \text{ETA(2)} - \text{E(2)N(3)}$$

The following can be done for every iz such that

$$N(iz) = \underbrace{\frac{G(iz) - A(iz)ETA(iz-1)}{B(iz) - A(iz)E(iz-1)}}_{ETA(iz)} - \underbrace{\frac{D(iz)}{B(iz) - A(iz)E(iz-1)}}_{E(iz)} N(iz+1)$$

Resulting in

N(w-2) = ETA(w-2) - E(w-2)N(w-1)

N(w-1) = ETA(w-1) - E(w-1)N(w)

The last expression will remain the same:

X(w)N(w-2) + A(w)N(w-1) + B(w)N(w) = G(w)

We can solve the last 3 equations by substitution, resulting in:

$$N(w) = \frac{G(w) + X(w)E(w-2)ETA(w-1) - X(w)ETA(w-2) - A(w)ETA(w-1)}{B(w) - A(w)E(w-1) + X(w)E(w-1)E(w-2)}$$

We can now solve the last equation as it only has one unknown. With a value of N at iz = w, we can now solve for N at iz = w-1. Similarly, a value can be solved for the previous N until iz = 1. A spreadsheet such as Microsoft Excel is most useful for this exercise and is enclosed as an attachment. After a value for N at each iz has been obtained, we can plot N versus iz. Additionally, plotting the log of N versus iz will indicate an overall removal efficiency.